Published in final edited form as:
Proteomics. 2009 May ; 9(9): 2503–2528. doi:10.1002/pmic.200800158.

Proteomic and selected metabolite analysis of grape berry tissues under well watered and water-deficit stress conditions

Jérôme Grimplet[1], **Matthew D. Wheatley**[1], **Hatem Ben Jouira**[2], **Laurent G. Deluc**[1], **Grant R. Cramer**[1], and **John C. Cushman**[1]

[1]Department of Biochemistry and Molecular Biology, MS 200 University of Nevada Reno. Reno, Nevada 89557-0200, USA

[2]Center of Biotechnology Borj Cédria B.P. 901, 2050 Hammam-Lif, Tunisia

Abstract

In order to investigate the unique contribution of individual wine grape (*Vitis vinifera*) berry tissues and water-deficit to wine quality traits, a survey of tissue-specific differences in protein and selected metabolites was conducted using pericarp (skin and pulp) and seeds of berries from vines grown under well watered and water-deficit stress conditions. Of 1,047 proteins surveyed from pericarp by 2D-PAGE, 90 identified proteins showed differential expression between the skin and pulp. Of 695 proteins surveyed from seed tissue, 163 were identified and revealed that the seed and pericarp proteomes were nearly completely distinct from one another. Water-deficit stress altered the abundance of approximately 7% of pericarp proteins, but had little effect on seed protein expression. Comparison of protein and available mRNA expression patterns showed that 32% pericarp and 69% seed proteins exhibited similar quantitative expression patterns indicating that protein accumulation patterns are strongly influenced by post-transcriptional processes. About half of the 32 metabolites surveyed showed tissue-specific differences in abundance with water-deficit stress affecting the accumulation seven of these compounds. These results provide novel insights into the likely tissue-specific origins and the influence of water deficit stress on the accumulation of key flavor and aroma compounds in wine.

Correspondence: Professor John C. Cushman, University of Nevada, Reno, Mail Stop 200, Reno, Nevada 89557-0200 jcushman@unr.edu**Fax:** +001-775-784-1650.

9 Supporting information

Additional Figure 1: 2D-PAGE analysis of *Vitis vinifera* cv. Cabernet Sauvignon berry pericarp proteins constant relative abundance in pulp and skin. Proteins that exhibited a non-significant ($p < 0.05$) change between the skin and pulp are indicated by circles and standard spot numbers on a representative gel. See Additional Table 5 for detailed listing of proteins.

Additional Table 1: Proteins whose abundance was significantly different between pulp and skin with corresponding mRNA expression.

Additional Table 2: Proteins whose abundance was significantly different between well watered and water-deficit in pulp with corresponding mRNA expression values.

Additional Table 3: Proteins whose abundance was significantly different between well watered and water-deficit in skin with corresponding mRNA expression values.

Additional Table 4: Proteins predominantly presented in seed with their corresponding mRNA expression values.

Additional Table 5: Proteins with constant relative abundance in pulp and skin.

Additional Table 6: Proteins also identified in Deytieux et al., 2007 [18], Giribaldi et al., 2007 [19], and Negri et al. 2008 [20].

Keywords

Vitis vinifera L; Water deficit stress; Tissue-specific proteins; Metabolites; Two-dimensional gel electrophoresis

1 Introduction

The berries of grape vine (*Vitis vinifera* L.) and related species are one of the most widely grown and economically most import fruit crops in the world. Since its initial domestication more than 7,000 years ago [1, 2], berries have been used for wine production, as well as grape juice, table grapes, raisins, and more recently for leaf, seed, and skin extracts by the nutraceutical and cosmetic industries [3, 4]. The genetic diversity of grapevine have been narrowed considerably by the selection of only a few familiar cultivars (e.g., Chardonnay, Cabernet Sauvignon, Syrah (Shiraz) and Merlot) now grown worldwide [1]. Quality traits, which are generally linked to a specific tissue, such as skin color due to the production of anthocyanins and proanthocyanidins, are controlled by relatively few genes [5, 6]. However, traits considered as desirable for one product could be undesirable for another. For example, seedlessness is a highly desirable trait in table grapes, however, seeds contain a high concentration of condensed tannins (i.e., proanthocyanidins), which are considered indispensable for conferring astringency and color stability to red wines [7]. The skin, pulp, and seed tissues of grape berries each confer unique properties to wine. The skin confers color, aroma, and other organoleptic properties of wine. The pulp contributes the majority of sugars, which are transformed into alcohol during the fermentation process. Skin and pulp tissues are the main source of volatile aroma compounds, such as terpenes, norisoprenoids, and thiols stored as sugar or amino acid conjugates [8]. The seed contains flavan-3-ol monomers and procyanidins (seed tannins), which contribute important organoleptic properties to wine [7].

Analysis of the protein composition of grape berries and must has been used to examine varietal and developmental differences as well as to analyze chemical and environmental effects in grape. Polyacrylamide gel electrophoresis (PAGE) analysis of must proteins has provided a means to readily identify different grape varieties [9]. Electrospray ionization-mass spectrometry (ESI-MS) has also been used to differentiate varieties by identifying different classes of pathogenesis-related (PR) proteins in grape juice [10]. In contrast, other researchers have concluded that one- and two-dimensional PAGE analysis of PR proteins was inadequate to readily differentiate varieties [11].

Protein extraction methods for mature grape berry clusters have been optimized with phenol-based methods being superior to TCA/acetone methods [12]. Proteomic comparison of ripe berry mesocarp from six different *Vitis* cultivars revealed that most 2D-PAGE profiles were ~70% similar to one another with the exception of a few proteins, such as alcohol dehydrogenase (ADH), which displayed large polymorphisms among the different cultivars [13]. High light and CO_2 concentrations apparently stabilized RuBisCO in grapevine plantlets as monitored by 1D- and 2D-PAGE and immunoblotting [14]. Herbicide stress on grapevine shoots, root, and leaves induced antioxidant and photorespiratory

enzymes, as well as a set of pathogenesis-related (PR) proteins [15]. Chronic salinity and water-deficit stress of grapevine shoots revealed distinct differences in protein expression patterns in cv. Chardonnay and cv. Cabernet Sauvignon [16]. *Vitis* leaves, in which alcohol dehydrogenase was over- or under-expressed, revealed abundance changes in carbon metabolism-associated proteins [17]. Analysis of grape berry skin proteins from cv. Cabernet Sauvignon at the beginning and end of véraision and in mature, harvest stage berries showed ripening-related protein abundance increases associated with anthocyanin biosynthesis and pathogen defense [18]. A similar, yet more comprehensive, analysis of berry ripening in *V. vinifera* cv. Nebbiolo Lampia showed that more than 100 proteins were differentially expressed during berry development [19]. More recently, analysis of changes in the expression of 67 grape skin proteins were monitored from véraison to fully ripe berries of *V. vinifera* cv. Barbera showing that many proteins with (a)biotic stress responses were developmentally regulated [20].

In order to better understand the complex transcriptional regulatory hierarchy controlling tissue-specific gene expression patterns, several studies have investigated the steady-state transcript abundance in discrete berry tissues. Large-scale expressed sequence tag (EST) sampling has been used to identify differences in expression associated with different organ and tissue types and developmental stages [21-23]. Large-scale mRNA expression profiling studies have investigated expression in flowers and developing berries of *V. vinifera* [24-27], in a fleshless berry mutant (cv. Ugni Blanc) [28], and in the skin of ripening berries of seven different *V. vinifera* cultivars [29]. More recently, large-scale mRNA expression profiles within skin, pulp, and seed tissues of well-watered and water-deficit stressed vines of Cabernet Sauvignon were surveyed using the GeneChip® *V. vinifera* (Grape) Genome Array [30]. However, no proteomic studies have been performed to investigate protein expression differences among different berry tissues.

In order to obtain information on protein expression changes in grape berry tissues in response to well watered and water-deficit stress conditions, a comparative 2D-PAGE analysis was performed using discrete tissue from the pericarp tissues (skin and pulp) and seed. Approximately 7% of the more than 1,000 skin and pulp proteins surveyed showed a two-fold or greater change in abundance in response to water deficit stress indicating that water-deficit stress can have a major impact on protein expression profiles in grape pericarp tissues. From the 695 seed proteins surveyed in the seed, seed protein expression patterns were completely distinct from those in the skin and pulp tissues, mainly due to high concentrations of seed storage proteins. Skin abundant proteins were associated mainly with the phenylpropanoid pathway, pathogenesis-related (PR) proteins, heat shock proteins, and polyphenol oxidase, whereas pulp abundant proteins included those involved in primary energy metabolism. Water deficit stress led to tissue-specific changes in protein expression. The skin showed increased abundance of proteosome, reactive oxygen detoxification enzymes, and selected enzymes involved in flavonoid biosynthesis, whereas pulp tissues showed increased in glutamate decarboxylase, PR proteins, and methionine synthase. Changes in the abundance of selected metabolites were also monitored in parallel with protein expression analysis. Tissue-specific and water status-dependent differences in metabolite profiles were also evident.

2 Material and methods

2.1 Plant material and growth conditions

Vitis vinifera L. cv. Cabernet Sauvignon berries were sampled on September 29, 2005, at which time the berries were fully ripe and corresponded to stage 38 (berry harvest) of the modified E-L system [31] from 20-year-old vines in the Shenandoah Vineyard (Amador County, CA, USA), stored on ice for 3 hours, frozen in liquid nitrogen and stored at −80° C. Therefore, it is possible that changes in the proteome and metabolome may have occurred during the time the berries were stored on ice. Pulp, skin and seeds were then separated without allowing berries to thaw. Skin was peeled off the pulp using a scalpel. The pulp was then cut into two halves from which the seeds were carefully removed. As complete removal of pulp cells from the skin or seed tissues was not possible, the observed differences in tissue-specific patterns reported here may show some residual contamination from pulp tissues. For the well-watered plants, irrigation was performed from E-L stage 27 [31]. Water deficit treated vines were never irrigated. Berry clusters were harvested from the sunny (Southern) side of the vine. Six biological replicates were collected and analyzed from both well watered and water-deficit treated vines.

2.2 Stem xylem water potential

Fully mature leaves were selected for stem water potential measurements [32]. A single leaf per plant was tightly zipped in a plastic bag to eliminate transpiration. Aluminum foil was then placed around the bag, deflecting light and heat. After two hours of equilibration time, the excised leaf was placed in a 3005 Plant Water Status Console pressure chamber (Soilmoisture Equipment Corp., Santa Barbara, CA, USA). The foil was removed before sealing the bagged leaf in the chamber. The balancing pressure required to visibly push stem xylem sap to the cut surface was recorded.

2.3 Brix assay

The Brix (total soluble solids) was assayed from juice crushed from harvested berries with a refractometer (BRIX30, Leica, Bannockburn, IL, USA).

2.4 Protein extraction

Protein extractions were performed in sets of 4 random samples, with the constraint that 2 biological replicates were never processed within the same set. Five g of skin or pulp tissue or 1 g of seed were ground to a fine powder in liquid nitrogen with mortar and pestle. Extraction was adapted from the phenol extraction protocol 4 as described [12], which was adapted from previously described protocols [33, 34]. Powder was vortexed in 10 mL of Sucrose Buffer 4 (0.7 M sucrose, 0.5 M Tris-HCl pH = 7.5, 50 mM EDTA, 0.1 M potassium chloride, 2 mM PMSF, 2% ß-ME, 1 Complete™ protease inhibitor cocktail tablet (Roche Diagnostics, Indianapolis, IN, USA), and 1% PVPP) and incubated for 10 min at 4° C. After incubation, an equal volume of 1 M Tris-saturated phenol (pH = 7.9) was added. The mixture was stored at −20° C for 30 min with vortexing every 10 min. The phases were separated by centrifugation (30 min at 0° C at 3,210 *x g*). The upper phenol phase was collected and re-extracted with an equal volume of Sucrose Buffer 4. Five volumes of 0.1 M

ammonium acetate in cold MeOH were added to the phenol phase to precipitate proteins, followed by incubation at −20° C overnight. The pellet was washed with 5 mL of cold 0.1 M ammonium acetate/MeOH 50:50 w/v, two times with 5 mL of cold acetone and once in 2 ml of cold acetone/ethanol 50:50 v/v. The pellet was then vacuum-dried 5 min and resolubilized in 1.5 ml of Rehydration Buffer (7 M urea, 2 M thiourea, 4% CHAPS, 10 mM DTT, 1% carrier ampholyte, pH = 5–7, and 1% carrier ampholyte, pH = 3–10). PVPP (50 mg) was added to each sample, then each sample was vortexed, and centrifuged (15 min at −4° C at 10,000 *x g*) and the supernatant was stored at −80° C.

2.5 Protein assays

Protein concentrations were determined using an EZQ™ Protein Quantitation Kit (Invitrogen, Carlsbad, CA, USA) with ovalbumin as a standard, according manufacturer's instructions. Concentration ranged from 3.6 mg/ml to 10.6 mg/ml.

2.6 2-DE and gel staining

In order to reduce technical variation, no more than 2 of the 6 replicates were processed within the same set of 2-D SDS-PAGE gels. The 2-D SDS-PAGE protocol was adapted from O'Farrell (1975) [35]. IEF was carried out using immobilized pH gradient (IPG) strips (24 cm, pH = 4–7, Immobiline™ DryStrip, GE Healthcare, Piscataway, NJ, USA). The loading volume used was 440 μL of protein extract, corresponding to a protein amount of 1.2 mg per strip. Protein IEF was performed using a Protean® IEF Cell (Bio-Rad, Hercules, CA, USA) at 20° C as follows: active rehydration at 50 V for 12 h, 200 V for 30 min with a linear increase in voltage, 500 V for 30 min with a linear increase in voltage, 1000 V for 1 h with a linear increase in voltage, and 10,000 V with a rapid increase in voltage until a total of 85,000 Vh had been reached. Strips were then stored at −20° C until further use. Once thawed, the strips were washed for 30 min in Equilibration Buffer (6 M urea, 30% glycerol, 2 M Tris-HCl pH 8.8, and 2% SDS) containing 1% w/v DTT followed by washing with Equilibration Buffer containing 2.5% w/v iodoacetamide for 30 min. SDS-PAGE was performed using non-commercial 12% polyacrylamide gels (18 cm × 20 cm × 1 mm) and run at 40 V for 2 h and 120 V for 15 h in a Bio-Rad Protean® II XL 2-D Multi-Cell. A Coomassie Brilliant Blue (CBB) G-250 procedure was used to stain the 2-D gels [36]. The gels were washed twice in 50% EtOH/2% phosphoric acid/deionized water (diH_2O) v/v/v for 1 h, then transferred to 2% phosphoric acid for 60 min, and finally allowed to shake for 3 days in 15% EtOH/17% ammonium sulfate/2% phosphoric acid/0.2% CBB G-250/dH2O v/w/v/w/v. The 2-D gels were imaged using a VersaDoc® Imaging System Model 1000 (Bio-Rad).

2.7 Protein identification

Spot excision was performed using the ProteomeWorks™ spot cutter (Bio-Rad); then trypsin digested according to [37] using the Investigator™ ProPrep™ (Genomic Solutions, Ann Arbor, MI, USA). The tryptic fragments were analyzed using an ABI 4700 Proteomics Analyzer (Applied Biosystems, Foster City, CA, USA) MALDI TOF/TOF™ mass spectrometer (MS). A 0.5 mL aliquot of a matrix solution containing 10 mg/mL alpha-cyano-4-hydroxycinnamic acid (Sigma-Aldrich, Inc., St. Louis, MO, USA) and 10 mM

ammonium phosphate (Sigma-Aldrich) in 70% acetonitrile was co-spotted with 0.5 mL of sample [38]. The data were acquired in reflector mode from a mass range of 700 to 4,000 Da, and 2,500 laser shots were averaged for each mass spectrum. Each sample was internally calibrated if both the 842.51 and 2211.10 ions from trypsin autolysis were present. When both ions were not found, the instrument used the default calibration. The eight most intense ions from the MS analysis, not present on the exclusion list, were subjected to MS/MS analysis. To this end, the mass range was 70 to precursor ion with a precursor window of 21–3 Da with an average of 5,000 laser shots for each spectrum. The resulting file was then searched by using automated MASCOT software (http://www.matrixscience.com/) through the IDQuest (Bio-Rad) interface was used for searching the NCBI nonredundant database (ver. 22_05_2007; 4,970,641 sequences), or the Contigs from Vitis Gene Index ver. 5.0 (ver. 18_9_2006, 23,871 sequences). Peptide tolerance was 20 ppm; 1 missed cleavage was allowed; MS/MS tolerance was 0.8 Da. The possibility of matching multiple translated isoforms was examined by manual analysis of peptides covering the sequences.

2.8 Statistical analysis

Results from 6 different gels were compared for well-watered and water-deficit-stressed vines for each tissue and the results of 12 different gels were compared between skin and pulp. Differences in spot abundance were statistically evaluated using the ANOVA method with geneANOVA software [39]. The number of detected spots showing differences with a P-value of ≤0.05 was then determined. The spots were counted as valuable if their normalized intensity was higher than 0.01% of the total spot intensity. However, for non-detected spots a background value was used in the gels where they did not appear in order to limit the rate of false positives. Average CV was calculated for each experiment with and without background values. Spots were identified and then curated manually with respect to spot quality (e.g., sharpness, resolution) and the quality of spot matching to reduce false positives.

For protein and mRNA abundance comparisons, Log_2 values of the protein and mRNA ratios between pulp and skin values were plotted and the regression curve was determined using Excel. The mRNA expression values determined by microarray expression profiling were obtained from [30]. The proteome analysis reported here was performed using berries harvested one year later from the same vines at the same harvest date as were used for mRNA profiling.

2.9 Metabolite extraction and derivatization protocol

Polar metabolites were extracted and derivatized with a water/chloroform protocol according to previously described procedures [40]. Freeze-dried berry tissue (6 mg) was placed in a standard screw-cap-threaded, glass vial. Samples were incubated in HPLC grade chloroform for 1 hour at 50°C in an oven. A volume of Millipore NANOpure™ water containing 12.5 mg L^{-1} of ribitol as an internal standard was added to each sample, and then incubated for an additional hour at 50°C. Finally, vials were allowed to cool to room temperature and then spun at 2,900 *x* g for 30 min. One mL of the polar phase was dried down in a vacuum concentrator overnight. Polar samples were derivatized by the addition of

120 μL of 15 mg mL^{-1} of methoxyamine HCl in pyridine, sonicated for 30 min, and incubated at 50° C for 1 h. 120 μL of MSTFA + 1% TMCS were added, incubated at 50° C for 1 h, and analyzed immediately with a PolarisQ™ 230 GC-MS (Thermo Fisher Scientific, Inc., Waltham, MA, USA). Derivatized samples (120 μL) were transferred to a 200 μL silanized vial insert and run at an injection split of 200:1 to bring the large peaks to a concentration within the range of the detector and 10:1 for detection of lower peaks. The inlet and transfer lines were held at 240° C and 320° C, respectively. Separation was achieved with a temperature program of 80° C for 3 min, then ramped at 5° C min^{-1} to 315° C and held for 17 min, using a 60 m DB-5MS column (J&W Scientific, 0.25 mm ID, 0.25 μm film thickness) and a constant flow of 1.0 ml min^{-1}. All organic acids, sugars and amino acids were verified with standards purchased from Sigma-Aldrich, Inc.

2.10 Metabolite data processing

Metabolites were identified in the chromatograms using two different software packages: AMDIS (ver. 2.64, United States Department of Defense, USA) and Xcalibur (ver. 1.3; Thermo Fisher Scientific, Inc.). The software matched the mass spectrum in each peak against three different metabolite libraries : NIST ver. 2.0 library (http://www.nist.gov/srd/), T_MSRI_ID library of the Golm Metabolome Database [41], and a local database containing more than 50 standards. Quantification of the area of the chromatogram peaks was determined using Xcalibur and normalized as a ratio of the area of the peak of the ribitol internal standard.

3 Results

3.1 Physiological data

Fully ripe berry samples were harvested from E-L stage 38 berries [31]. This harvest date corresponded to the time of commercial harvest of the vineyard. Stem water potential differences were monitored for well-watered and water-deficit treated vines as a comprehensive indicator of water-deficit in the vines [42]. Stem water potentials were significantly more negative for water-deficit treated vines than for well-watered vines at the time of harvest (Table 1). Brix values, an approximate measure of the mass ratio of dissolved solids to water in fruit juices, were also significantly different between berries harvested from well-watered and water-deficit-stress treated vines. These values are close to the generally recommended value (23° Brix) for harvest of cv. Cabernet Sauvignon in central California. However, no significant differences in berry diameter were observed (Table 1).

3.2 Comparative 2D-PAGE analyses of berry tissue proteins

Three different berry tissues (i.e., skin, pulp, and seed) were dissected manually as a starting point for 2D-PAGE analysis. A relatively large number of biological sample replicates (six) for each tissue type and water status treatment were performed to obtain a statistically robust assessment of the differences in protein expression patterns. Each replicate was considered a biological replicate because it was collected from a different vine. Replicate samples were extracted and analyzed such that no more than 2 gels from the same tissue/condition were processed at the same time within the same set of samples. In total, 1,047 spots were

detected in skin and pulp from vines subjected to either well watered or water-deficit stress conditions (Table 2). For these two tissues, an average of 854 spots per gel with an intensity value greater than 0.01% of the total average spot intensity was detected. In contrast, seeds presented a totally different profile that was not directly comparable to the skin and pulp tissue profiles. Therefore, 2D-PAGE gels for this tissue were processed independently until final spot matching. In seeds, a total of 695 spots was detected in seeds from vines subjected to either well watered or water-deficit stress conditions (Table 2). An average of 605 spots per gel with intensities higher than 0.01% of the total spots intensity was detected. To maximize the number of proteins identified in this study, such as transcription factor or hormone metabolism-related proteins that typically are of low abundance, faint spots were included, not only leading to a relatively high number of spots per gels (Table 2), but also a relatively high average coefficient of variation (CV). However, these CV values were within a range that was consistent with previously reported average or mean values for other plant proteomic analyses (0.26-0.31 [43]; 0.47-0.75 [44]; and 0.24 [45]). The decision to retain background values tended also to increase CV values.

In order to identify differentially expressed proteins among the three different berry tissues, 2D-PAGE gels were compared. Spots that displayed differential abundance after ANOVA ($p<0.05$) and a two-fold ratio or greater difference were identified and then curated manually with respect to spot quality (e.g., sharpness, resolution) and the quality of spot-matching to reduced false positives. Analysis of pericarp proteins revealed 90 spots that displayed differential abundance after ANOVA ($p<0.05$) and a two-fold ratio or greater difference: 54 were more abundant in the skin (Fig. 1 and Table 3) and 36 were more abundant in the pulp (Fig. 2 and Table 3). A majority of proteins (217 in total) showed a relatively constant abundance between the skin and pulp (see Additional Figure 1 and Additional Table 5).

Because of the low number of proteins that could be matched between seed and the pericarp tissues, no statistical analysis could be performed. Therefore, proteins were considered to be specific to the seed if their abundance was: 1) higher than 0.1% of the total spot intensity and 2) two-fold or greater more abundant than the spots localized at the same position on pericarp gels. Using these criteria, 163 seed protein spots were identified (Fig. 3 and Table 4), including 19 spots that matched protein spots present within pericarp tissues. A reciprocal comparative analysis could not be performed because of the relative over abundance of storage proteins in seed compared with pericarp tissues, which significantly reduced the relative abundance of other proteins.

3.3 Identification of differentially expressed proteins among tissues

Protein spots that displayed differential abundance after ANOVA ($p<0.05$) and a two-fold or greater ratio threshold filtering were eluted from representative 2-D gels, digested with trypsin and analyzed by MALDI TOF/TOF tandem mass spectrometry. Within pericarp tissues comparison, 47 of 54 protein spots that were more abundant in skin and 18 of 36 protein spots more abundant in pulp were identified (Table 3). Proteins expressed in the skin with functions related to phenylpropanoid and amino acid biosynthesis, light and dark reactions of photosynthesis, biotic stress responses (e.g., pathogenesis-related (PR) proteins) and heat shock proteins, were much more abundant relative to pulp proteins. In contrast,

pulp tissues showed high abundance of proteins with functions in reactive oxygen scavenging (ROS), ripening-related proteins (e.g., grip22), abiotic stress response (e.g., stress-induced proteins and dehydrins), and several unknown or hypothetical proteins (Table 3).

In seeds, a majority of spots (130/163 or 80%) spots analyzed as being abundant (>0.1% of the total spot intensity) and two-fold or greater more abundant than in pericarp tissues could be assigned functions based on MS data (Table 4). Of those proteins assigned a function, a majority (94/130 or 72%) was identified as globular or other seed storage proteins, seed maturation or late embryogenesis abundant proteins. Other classes of proteins included those with functions in carbohydrate or energy metabolism, protein fate, and biotic or abiotic stress responses (Table 4).

3.4 Comparative 2D-PAGE analyses of berry proteins in response to water-deficit stress

Water deficit irrigation treatment is known to alter the composition of grapevine berries [46] and reduce leaf area and photosynthesis within the canopy [47]. Water deficit stress can also have profound effects on the mRNA abundance within different berry tissues [30]. In order to determine if water deficit causes corresponding changes in protein composition within the berry, we analyzed the protein profiles of berry tissues collected from grapevines that were well watered or water-deficit stressed. Spots that displayed differential abundance after ANOVA ($p<0.05$) and a two-fold ratio or greater difference were identified and then curated manually to reduce false positives. Analysis of skin proteins revealed 31 spots that showed significantly different abundance upon water stress treatment (14 in well-watered; 17 in water-deficit treated). After manual curation, 18 spots were identified: 9 were more abundant in the well-watered berries (Fig. 4A and Table 5) and 9 were more abundant in water-deficit-stressed berries (Fig. 4B and Table 5). Analysis of pulp tissue identified 28 spots with significantly different abundance upon water stress treatment (18 in well-watered; 10 in water-deficit treated). After manual curation, 12 spots were identified: 7 were more abundant in the well-watered berries (Fig. 4C and Table 6) and 5 were more abundant in water-deficit-stressed berries (Fig. 4D and Table 6). Analysis of seed proteins revealed only 6 spots that showed significantly different abundance in the seed upon water stress treatment (5 in well-watered; 1 in water-deficit treated). After manual curation, only 1 spot (SSP:7203, TC58896), which encoded a vacuolar H^+-ATPase subunit E, was identified that was more abundant in the well-watered berries (Fig. 3 inset, Table 4).

3.5 Identification of differentially expressed proteins in response to water-deficit stress

Protein spots that displayed differential abundance after ANOVA ($p<0.05$) and a two-fold or greater ratio threshold filtering were eluted and analyzed as described above. Within skin tissue, 9 of 9 protein spots that were more abundant under water deficit stress and 5 of 9 protein spots more abundant under well-watered conditions were identified successfully (Table 5). Within pulp tissue, 4 of 5 protein spots that were more abundant under water deficit stress and 5 of 7 protein spots more abundant under well-watered conditions were identified successfully (Table 6). The constellation of water-deficit stress-induced proteins was completely distinct for each of these two tissues. However, the skin displayed a notable increase in the relative abundance of proteosome subunits and peptidases and the ROS

scavenging enzyme, cytosolic ascorbate peroxidase, whereas the pulp showed increases in isoflavone reductase, glutamate decarboxylase and an endochitinase. In contrast, water-deficit had little effect on the expression of seed proteins.

3.6 Correlation of mRNA and protein expression patterns

Protein abundance changes within tissues and in response to water-deficit stress were compared with mRNA changes within the same berry tissues [30]. MALDI TOF/TOF MS/MS identification results were analyzed carefully in order to match accurately a protein identity with a specific member of a gene family within a multigene family. From the 65 identified proteins in the skin/pulp comparison, the possibility of matching to more than one mRNA could not be ruled out for four proteins spots. For eight proteins, comparison with mRNA could not be performed because corresponding probe sets for mRNA expression data were not present on the GeneChip® *Vitis* Genome Array (Affymetrix®) (see Additional Table 1). For identified proteins exhibiting tissue-specific expression patterns, 47 of 57 (82%) had a corresponding mRNAs expression pattern that was preferentially expressed in the same tissue as their protein counterpart. These data indicate a rather good qualitative correlation between mRNA and protein expression patterns in general. However, only 18 of 57 (32%) of these proteins exhibited a corresponding two-fold or greater ratio of differential expression at both the mRNA and protein levels. The Pearson correlation coefficient between quantitative protein and mRNA abundance $\log_2$ difference ratios for the entire pericarp data set was 0.216 (Fig. 5A). The Pearson correlation coefficient between protein and mRNA abundance $\log_2$ difference ratios for the seed vs. pericarp was only 0.017 (Fig. 5B). These data indicate a poor overall correlation between mRNA and protein expression patterns for genes expressed preferentially within a specific tissue.

In the water status comparisons of skin and pulp tissues, 2 of the 23 identified spots did not have a mRNA counterpart on the microarray chips, and 11/21 (52%) of proteins showed agreement with the general trend of mRNA expression in response to water-deficit stress treatment (see Additional Tables 2 and 3). However, none of the transcripts displayed a two-fold or greater ratio difference in expression.

In the seed/pericarp comparison, of the 132 proteins identified, corresponding mRNA expression data were available for 77 proteins. Of these, 62 of 77 (81%) mRNA were expressed preferentially in the seed and a majority, 53 of 77 (69%) presented a twofold or greater ratio difference in both protein and mRNA (see Additional Table 4).

3.7 Metabolite analysis

In order to explore possible relationships between protein abundance and metabolite accumulation in different berry tissue, the relative abundance of polar metabolites was analyzed by GC-MS. Large differences in the relative abundance of selected metabolites were found among the different tissues. For example, 6/13 amino acids, 6/13 organic acids and 6/6 sugars analyzed shown significant differences in abundance among skin, pulp and seed tissues (Fig. 6). The effect of water deficit on the accumulation of selected metabolites was also determined. Catechin, sucrose and alanine were more abundant in the pulp of

berries from water-deficit treated vines, whereas glutamate and tartrate were more abundant in the pulp of berries from well-watered vines (Figure 7).

4 Discussion

We have performed the first survey of tissue-specific protein expression patterns within pericarp tissues (skin and pulp) and seed tissues of grape berries from grapevines subjected to well watered and water-deficit stress conditions. Although previous studies have reported proteomic analysis of grape berry skin proteins [18, 20] or whole berries at various times during berry development [19], none have investigated tissue-specific protein expression patterns. Our survey of a total of 1,047 spots (average of 854) from pericarp tissues (skin and pulp) revealed that while most proteins showed a relatively constant expression between skin and pulp, 90 (8.6%) spots exhibited a two-fold ratio or greater difference in tissue expression (Fig. 1 and 2 and Table 3). Furthermore, our survey of a total of 695 spots (average of 605) from seed tissues indicated that seeds presented a proteome that was completely distinct from that of the pericarp, mainly due to high concentrations of seed storage proteins (Fig. 3 and Table 4). A comparison of our results with recent reports of skin-specific [18, 20] or pericarp [19] proteomic analyses of wine grape berries indicated generally strong agreement skin-specific protein expression patterns with only a few exceptions (e.g., isoflavone reductase and methionine synthase) (Additional Table 6). In most cases, tissue-specific enzyme localization was in general agreement with substrate localization as might be expected.

4.1 Phenylpropanoid pathway

All identified proteins with functions in the phenylpropanoid pathway (Table 3) showed expression specific to the skin consistent with their mRNA expression profiles [30, 48]. Phenolic compounds are major wine constituents responsible for organoleptic properties such as color and astringency. Moreover, a majority of phenolic compounds in wine are derived from flavonoids (e.g., tannins, anthocyanins). For red grapes, roughly 30-40% of the total phenolic content is located in the skins and 60-70% in the seeds [49]. All of the identified spots in this functional group, with the exception of caffeoyl-CoA O-methyltransferase (SSP:5206, TC70299), correspond to enzymes with functions in the latter steps of anthocyanin biosynthesis (Figure 8). This caffeoyl-CoA O-methyltransferase is likely to be involved in anthocyanin methylation as a closely related methyltransferase from *Mesembryanthemum crystallinum* was specific for flavonoids in addition to caffeoyl-CoA [50]. The corresponding mRNA for this enzyme is also preferentially expressed in the skin [30] or pericarp of red wine grape varieties [48]. The expression of chalcone isomerase (SSP:3210, TC55034), which is a key enzyme of the anthocyanin biosynthetic pathway, was also mainly in the skin, consistent with its mRNA expression pattern [30]. Similarly, the anthocyanin biosynthetic enzymes, flavonone-3-hydroxylase (SSP:4405, TC70298) and leucoanthocyanidin dioxygenase (SSP:5411; TC69652), exhibited skin-specific mRNA and protein expression patterns (Table 3). Both of these enzymes showed increased protein abundance following véraison in cv. Cabernet Sauvignon [18]. UDP-glucose:flavonol-3-O-glucosyltransferasae (UFGT, SSP:7411, AF000371) mRNA was also expressed specifically in the skin [51]. This enzyme plays a critical role in anthocyanin accumulation as

retrotransposon-induced mutation of the MYB transcription factor (VvmybA1) gene [52] leading to its expression impairs anthocyanin accumulation in red grape varieties [53] with this mutation being common to many white grape varieties [5]. The enzymatic activity of recombinant UFGT has been documented *in vitro* [54]. Two isoforms of UFGT were found to accumulate preferentially following véraision in cv. Cabernet Sauvignon [18]. Two isozymes of glutathione-S-transferase (GST) (SSP:3103, TC58036 and SSP:6101, TC69505), which also showed skin-specific mRNA and protein expression, play a critical role in the final step of anthocyanin accumulation by conjugating glutathione to cyanidin glucoside, which is then transported into the vacuole [55]. mRNA encoding GST was more abundant in red versus white grape skin [48]. The 5' flanking promoter regions of both UFGT and GST genes share MYB cis-element binding domain sites [56], indicating that the relative mRNA and protein expression of both genes may be coordinately regulated. Lastly, an isoflavone reductase (SSP:8302, TC52848), which is involved in isoflavonoid phytoalexin biosynthesis [57], was more abundantly expressed in the pulp than in the skin, which is also in accordance to its mRNA profile [30]. Overall, most flavonoid biosynthetic enzymes identified were found to be localized to the skin (Figure 8), consistent with known expression patterns and previous proteomic analysis of berry skins (Additional Table 6).

Metabolite analyses revealed tissue-specific differences in the relative abundance of selected compounds. For example, caffeic acid exhibited specific expression in the skin (Figure 6A). This precursor metabolite is a possible substrate of caffeoyl-CoA O-methyltransferase (SSP: 5206), whose mRNA [30] and protein (Table 3) are also expressed preferentially in the skin. Alternatively, this enzyme may be specific for flavonoid as mentioned above. Catechine, a flavonoid, was significantly more abundant in seed (Figure 6A) and in water-deficit stressed berries (Figure 7), consistent with the mRNA expression pattern of leucoanthocyanin reductase in these tissues [30], however, this biosynthetic enzyme was not identified in this study. The tissue-specific expression patterns of key phenylpropanoid enzymes established here will be critical to rational manipulation of the expression of these enzymes in the future.

4.2 Amino acid metabolism

Nitrogen is mainly incorporated into the berry through glutamine synthetase/glutamate synthase. Two isoforms of glutamine synthetase (SSP:3305, TC60125 and SSP:5303, 64127) were identified as homologues of cytosolic glutamine synthetase, which catalyze glutamine synthesis using glutamate, a key nitrogen reserve in plants. Cytosolic isoforms of this enzyme have been detected in vascular tissues of grape berry pulp [58] and in berry skins where the protein was found to be 3.5 times more abundant prevéraison than postvéraison [18]. This phloem-specific expression pattern indicates that the cytosolic glutamine synthetase isoenzyme functions to generate glutamine for intercellular nitrogen transport [59]. The higher abundance of both enzymes in the skin (Table 3) probably reflects the higher percentage of vascular tissues within berry skin. Glutamate also appeared to be slightly more abundant in the skin (Fig. 6), although this difference was not significant and significantly less abundant in pulp following water-deficit stress (Figure 7).

Homocysteine S-methyltransferase (SSP:4318; TC55907), which catalyzes the last step of methionine biosynthesis, was highly abundant in the pulp. This pattern of enzyme expression would predict that methionine content would be higher in the pulp than in the skin, although no direct metabolite data are available to confirm this prediction. Methionine is metabolized during malolactic fermentation into various sulfur compounds [60]. Methionine content is well correlated with the abundance of the volatile compound methionol (3-(methylthio)-propanol), which has a raw-potato odor, in fermented must [61]. In contrast, S-adenosylmethionine (SAM) synthetase (SSP:4413, TC51748), which catalyzes the first step of methionine degradation, was highly abundant in the skin. SAM synthetase may participate in the production of aromatic compounds requiring methylation, such as 2-methoxy-3-alkylpyrazine or 2-hydroxy-3-alkylpyrazine, in the skin [62]. Alternatively, SAM synthetase may be required for lignin biosynthesis, as caffeoyl-CoA O-methyltransferase (SSP:5206), which was also more abundant in the skin, requires SAM as a co-factor.

Proline is the most abundant amino acid in grape berry, specifically in cv. Cabernet Sauvignon, and accumulates to high levels during the later stages of fruit ripening. Proline is synthesized from glutamate by delta 1-pyrroline-5-carboxylate synthetase (P5CS), which is localized mainly in pericarp tissue [63]. Proline was found to accumulate predominantly in skin and pulp tissues (Fig. 6B), consistent with the subcellular localization of P5CS. Like proline, threonine is clearly more abundant in pericarp rather than seed tissues. Threonine levels in must are strongly correlated with the accumulation of odorants related to fatty acid synthesis including, ethyl acetate, ethyl butyrate, and hexanoic and octanoic acids and longer chain alcohols such as isoamyl alcohol and β-phenylethanol [61].

Shikimic acid, which is an important precursor of aromatic amino acids, was most abundant in skin, less abundant in the pulp, and least abundant in the seed (Fig. 6B). Shikimic acid is thought to serve as the major source of precursors for two groups of important wine aromatic compounds that include volatile phenols and vanillin [64]. These results provide novel insights into the probable tissue-specific origins of key flavor and aroma compounds in wine.

4.3 Energy

Two proteins with energy-related functions were expressed preferentially in the pulp: a cytosolic inorganic pyrophosphatase (SSP:3114, TC56801) and a plastic fructosebisphosphate aldolase (SSP:8303, TC52261). Inorganic pyrophosphatase catalyzes the hydrolysis of pyrophosphate (PPi), which is formed principally as the product of the many biosynthetic reactions that utilize ATP. In the pulp, its function is probably related to regulation of inorganic pyrophosphate in the cytosol [65]. Fructose-bisphosphate aldolase is a glycolytic enzyme that catalyses the reversible aldol cleavage or condensation of fructose-1,6-bisphosphate into dihydroxyacetone-phosphate and glyceraldehyde 3-phosphate and is abundant in the pulp, but not the seeds of ripe berries [58].

The remaining proteins with functions related to energy production and photosynthesis were preferentially expressed in berry skin. These included ATP synthase beta subunit (SSP:3503, TC63054) and cytochrome *c* oxidase (COX), subunit 6b-1 (SSP:203, 204; TC51789), the

terminal enzyme of the respiratory chain that oxidizes cytochrome *c* and transfers electrons to molecular oxygen to form molecular water. During berry development, transcripts encoding proteins with photosynthesis-related functions are most strongly expressed at flowering and two-weeks after flowering and then decline steadily in abundance throughout berry development [24, 25]. However, the skin of ripe berries still contained detectable amounts of proteins with functions related to photosynthesis and carbon assimilation. For example, several light harvesting components (Chlorophyll a-b binding protein (SSP:4120, TC62932), photosystem II components (Oxygen evolving enhancer protein 1 (SSP:2218, TC53930; SSP:3207, TC54765) and enzymes involved in carbon fixation including the large subunit of RuBisCO (ribulose-1,5-bisphosphate carboxylase/oxygenase) (SSP:8504, TC57584); RuBisCO subunit binding-protein alpha (SSP:1621, TC67963) and transketolase 1 (SSP:6727, SSP:6729; TC52655) were more abundant in the skin than in the pulp (Table 3). RuBisCO has been detected in skin [18], but was reported to be in very low abundance in the pulp of mature berries [58]. Transketolase has also been reportedly expressed in berry skin and shown to increase in abundance late in berry ripening [20] (Additional Table 6), possibly to supply carbon skeletons for biosynthetic pathways operating in this tissue during ripening. The expression pattern of photosystem and carbon assimilation proteins indicates that the skin might retain a functional photosynthetic apparatus or its remnants undergoing degradation in mature berries.

4.4 Biotic and abiotic stress responses

Grape ripening-related proteins (GRIPs) are abundant in postvéraison ripening berries [66]. Grip22-related proteins, which have been identified to be allergens in Kiwi [67], were found to be expressed in either the pulp (SSP:3111, TC55027) or the skin (SSP:7108, TC55027). However, the corresponding transcript for this protein showed no tissue-specific expression (Table 3). These two Grip22 proteins did differ in their experimentally determined pI, suggesting tissue-specific posttranslational modification. GRIP homologs in Kiwi are known to undergo glycosylation, which may be critical for the allergenic potential of these proteins [68, 69]. A second allergenic protein (SSP:1009, TC65039), which was more abundant in the pulp, and identified as a major allergen in cherry [70], is actually a pathogenesis-related (PR) protein (Table 3). Two skin-abundant PR proteins (SSP:7104, SSP:7105; TC68949) were also identified as PR10 proteins and are probably different products encoded by the same gene as judged by their relative proximity within the gel. PR10 has been observed previously to be expressed in mature berry skin [18] and increased in abundance during the later stages of ripening and are thought to play a role in berry protection [20]. SSP:4006 (TC58333) corresponds to a PR4 protein, which known to have antifungal activity [71], and thus may also contribute to berry protection. Another PR protein, β-1,3 glucanase (SSP: 6212, TC61082), which is induced by fungal pathogen treatment [72], was found to be most abundant in skin tissue (Table 3) as was the corresponding transcript encoding this protein [30]. β-1,3 glucanases have also been found to increase in activity [18] and protein abundance during berry ripening in skin tissue [19, 20] (Additional Table 6).

A number of heat shock proteins (HSPs) were also found in the skin. SSP1706 (TC54161) was found to be a close homologue of a watermelon HSP70 [73]. Unfortunately, no peptides corresponded with N-terminal transit peptide of the grape homologue, so the subcellular

location of this protein cannot be predicted. A second HSP (SSP:3719, TC53932) corresponds to a tobacco HSP90, which has been shown to play a key role in the conformational regulation of R protein recognition complexes and viral resistance [74]. Various other classes of HSPs, including multiple HSP70 isoforms have been described in grape berries [19] (Additional Table 6).

Preventing oxidative browning of grapes caused by polyphenol oxidase (PPO) is a major concern for the dry fruit industry and the production of white wine [75]. SSP:1012 (TC51691), which corresponds to a polyphenol oxidase gene described previously [76], was most abundant in the skin consistent with an earlier report that confirmed that grape berry skins contain high amounts of PPO activity [77]. However, more abundant isoforms (SSP: 1004, SSP:1007; TC51691) of PPO were identified (see Additional Table 5), but these did not show differential abundance among berry tissues. Several PPO isoforms are abundantly expressed in berry skins at véraison [20] and then their abundance declines towards ripening [19, 20] (Additional Table 6). Members of another class of stress proteins, the late embryogenesis abundant (LEA) proteins (SSP:1403, SSP:2518), exhibited pulp-specific expression patterns. These proteins belong to the SK_n group of acidic dehydrins [78]. The apparent molecular weight of these two proteins is higher than predicted consistent with previous observations for this group of proteins [79]. A late embryogenesis protein was also reported previously to be expressed in berry skin [20].

4.5 Organic acids

Tartrate is one of the most abundant organic acids in grape berries. The enzyme catalyzing the formation of tartrate (L-idonate dehydrogenase) in berries has been recently identified and belongs to the ascorbic acid degradation pathway [80]. The innermost region of the berry pulp surrounding the seed has been shown to contain the highest tartrate concentrations, but seeds were not assayed directly by these authors [81]. We observed that tartrate is significantly less abundant in the seed than in surrounding tissues (Figure 6C), despite the observation that transcripts for L-idonate dehydrogenase are most abundant in seeds [30]. More detailed analysis of the expression of the genes and corresponding enzymes that participate in tartrate biosynthesis is needed. The detection of high concentrations of threonate in the pulp of berries (Figure 6C) also reinforces the hypothesis that ascorbate is metabolized into oxalate and threonate in grape although the catalyzing enzyme remains unknown [82]. Malate, like tartrate, is among the most abundant organic acids and the major determinant of titratable acidity in berries. Malate was more abundant in the pericarp than in the seed consistent with previous results [81] and the relative transcript abundance for malate biosynthetic enzymes [30]. Succinate was also more abundant in the skin than in pulp, as was succinate dehydrogenase (SSP:5704, TC51756)) (Table 3). Succinate has not been detected previously in grape berry juice [83], likely due to the difference in detection methods employed and the low relative abundance of succinate, which is about 100-fold less abundant than the major organic acids.

4.6 Carbohydrates

The major forms of stored carbohydrates in berries are glucose and fructose, which are derived mainly from sucrose exported from the leaf and transported in the phloem to the

berry cluster [84] or derived from starch reserves within the berry itself [27]. This study confirmed these previous observations as pulp and skin accumulated much larger amounts of fructose and glucose than sucrose (Figure 6D). In contrast, seed tissues accumulated more sucrose than glucose and fructose (Figure 6D) consistent with earlier observations [85]. Gluconate, which can be metabolized via the oxidative pentose phosphate pathway in plants [86], is more abundant in skin than in pulp and seed (Figure 6D). High concentrations of gluconate can cause severe problems in winemaking processes including the control of alcoholic fermentation, biological aging, and stability [87]. Trehalose was found predominantly in the seed and skin (Figure 6D) where it may function as an osmoprotectant in these tissues or play roles in cell wall structure, cell division, glycolysis and starch accumulation [88]. In grape berry, trehalose phosphate synthase (1608440_at; TC48283) tissue-specific mRNA accumulation showed a similar pattern with trehalose itself [30].

4.7 Water-deficit stress responses

Approximately 7% of all skin and pulp proteins showed a two-fold or greater change in abundance in response to water deficit stress (Tables 5 and 6; Additional Tables 2 and 3) indicating that water-deficit stress can have a major impact on protein expression profiles in grape pericarp tissues. In skin, there was an apparent increase in the abundance of proteosome alpha (SSP4204, TC54618) and beta (SSP:5109, TC68818) subunits and several peptidases (Table 5), indicating that water-deficit stress is likely to increase protein turnover in the berry. Induction of multiple proteosome subunits in response to water-deficit stress has been observed previously in grapevine leaves [16]. Skin tissue also exhibited an increased abundance of cytosolic ascorbate peroxidase (SSP:5215, TC51718). Water-deficit stress is known to increase the mRNA expression of cytosolic ascorbate peroxidase in various plant species, including cowpea, where it is responsible for H_2O_2 detoxification and protection against oxidative stress [89].

In contrast, some proteins appeared more abundant in skin of berries from well-watered vines. For example, two isozymes involved in flavonoid biosynthesis, chalcone isomerase (SSP:3220, TC55034) and leucoanthocyanin dioxygenase (SSP:5501, TC69652) were significantly more abundance in well-watered vines (Table 5). Interestingly, a second, skin-specific isozyme of chalcone isomerase (SSP:3210) and leucoanthocyanin dioxygenase (SSP:5411), respectively, showed no significant change in abundance following water deficit stress. Water deficit causes an increase in the mRNA of most flavonoid biosynthetic enzymes [30, 90, 91] and an increase in flavonoid content of both berries and wine [46, 90, 91]. These secondary isozymes are likely to fulfill flavonoid biosynthesis demands under water-deficit conditions demonstrating the existence of a division of labor between these different isozymes depending on water status.

In contrast, pulp tissues exhibited a completely different set of proteins with differential expression to water-deficit stress (Table 6). For example glutamate decarboxylase (SSP: 5619; TC54345), which catalyzes the decarboxylation of L-glutamate to form gamma-aminobutyrate (GABA) and CO_2 [92], was more abundant and glutamate accumulation declined significantly under water-deficit stress (Figure 7). Interestingly, the product of this reaction, GABA, has been observed to be more abundant under water-deficit tissues of green

coffee beans [93] and tomato suspension cells which led to increased rates of glutamate decarboxylation into alanine and GABA [94]. The observed reduction of glutamate abundance and increase in alanine under water stress (Figure 7) in grape berry pulp indicates that glutamate decarboxylase is also involved in metabolic adjustments under water stress in grape berry pulp. In contrast, no change in glutamate abundance was observed in the skin following water-deficit stress. In addition, the large increases in myo-inositol and sucrose observed under water deficit stress (Figure 7) probably reflect their respective roles as osmoprotectants and precursors for the formation of raffinose series sugars, which are critical to enhanced water-deficit stress tolerance [95]. A class IV endochitinase (SSP:3113, TC68794) was also induced by water-deficit stress as is commonly observed for many other PR proteins. This class of protein was shown previously to accumulate during the later stages of berry ripening to high concentrations [96]. The observed increase in shikimate in pulp under water-deficit stress may be related to an increase of shikimate derived volatile compounds as well as tannins, flavonoids, and lignans [97].

Several other pulp proteins were significantly enhanced in their expression under well-watered conditions including methionine synthase (SSP:6715, TC52137), which catalyzes the transfer of a methyl group from 5-methyltetrahydrofolate to homocysteine resulting in methionine formation. UDP-glucose pyrophosphorylase (UGP, SSP:8602, TC57645) abundance was significantly higher in pulp from well-watered vines. UGP catalyzes the formation of UDP-glucose from the phosphorylation of glucose-1-phosphate and participates in the biosynthesis of carbohydrates and cellulose in sink tissues [98]. In grape leaves, increased UGP abundance was correlated with a decrease of sucrose abundance [17], as was observed here.

4.8 mRNA and protein expression correlation

Comparison of mRNA and protein expression patterns between the skin and pulp revealed that most proteins (82%) showed the same tissue-preferential expression pattern, as did their corresponding mRNAs with a Pearson correlation coefficient of 0.46. These data indicate only a moderate correlation between mRNA and protein expression patterns in these tissues. However, if the magnitude of tissue-specific expression were considered at the two-fold or greater ratio of differential expression for both mRNA and protein levels, then only 32% of proteins showed similar patterns of expression between these two tissues with a Pearson correlation coefficient between protein and mRNA abundance $\log_2$ difference ratios of 0.216 (Fig. 5A).

Comparison of mRNA and protein expression patterns between the seed and pericarp also revealed that most proteins (81%) showed the same tissue-preferential expression patterns. In contrast to pericarp tissues, however, a majority of seed proteins (69%) presented a two-fold or greater ratio difference in both protein and mRNA relative abundance. However, the Pearson correlation coefficient between protein and mRNA abundance $\log_2$ difference ratios for the seed vs. pericarp was only 0.017 (Fig. 5B). These data indicate a rather poor correlation between mRNA and protein expression patterns for genes expressed preferentially within a specific tissue. About half (52%) of pericarp proteins showed the same water-status-dependent trend in expression as did their corresponding mRNAs,

however, none of the transcripts/protein comparisons displayed a two-fold or greater difference in expression.

Other studies comparing relative protein abundance with relative transcript abundance estimated by EST counting, northern blotting, or microarray expression profiling generally showed a moderate to weak correlation (r = 0.50 or less) depending on the study [99-102]. Our results and results from these studies indicate that more than half of documented protein accumulation differences are determined after transcription via protein modifications, differential rates of translation, or differences in protein stability and turnover.

5 Concluding remarks

This large proteomic study has for the first time surveyed the tissue-specific differences in protein expression of mature wine grape (*Vitis vinifera*) berries. More than 1,700 protein spots were mapped by 2D PAGE and more than 250 proteins were identified by MALDI-MS/MS that showed tissue-specific expression among skin, pulp, and seed tissues. About 90 identified proteins showed differential expression between the skin and pulp and 163 identified proteins showed seed-specific expression. The skin was significantly enriched in proteins of the phenylpropanoid and amino acid biosynthesis pathways and photosynthesis and pathogenesis-related response proteins. In contrast, the seed proteome was completely distinct from that of the pericarp and was comprised largely of seed storage, maturation, or late embryogenesis abundant proteins. Comparison of tissue-specific protein expression patterns with available mRNA expression patterns revealed that a majority (81%-82%) of proteins showed qualitative, tissue-preferential expression pattern consistent with their corresponding mRNAs. However, relatively fewer pericarp (32%) or seed (69%) proteins showed similar patterns of quantitative expression among tissues. These results clearly indicate that protein accumulation patterns are strongly influenced by post-transcriptional processes in agreement with other large-scale proteome studies in plants.

The impact of water-deficit stress was also studied and found to have a profound influence on tissue-specific protein expression patterns resulting in significant changes in the expression of approximately 7% of pericarp proteins. Skin responses to water deficit stress were diverse with an obvious increase in the abundance of proteosome subunit proteins and proteases, reactive oxygen detoxification enzymes, and selected enzymes involved in flavonoid biosynthesis, whereas the pulp showed increases in isoflavone reductase, glutamate decarboxylase and an endochitinase. In contrast, water-deficit caused little effect on the expression of seed proteins as might be expected as the seeds in mature berries would be at the end of their developmentally programmed preparative phase for desiccation tolerance present in most orthodox seeds.

Finally, a limited survey of 32 metabolites by GC-MS showed that 18 exhibited tissue-specific differences in abundance with skins accumulating high concentrations of caffeic acid, proline, shikimate, and gluconate. Water-deficit stress caused increases in alanine, catechine, myo-inositol, shikimate and sucrose, but decreases in glutamate and tartrate in pulp tissue. Overall, these results provide many novel insights into the likely tissue-specific origins and the influence of water deficit stress on the tissue-specific accumulation of

enzymes that catalyze the formation of key flavor and aroma compounds in wine including organic acids, specific sugars, phenylpropanoids, proanthocyanins, and volatile compounds.

Supplementary Material

Refer to Web version on PubMed Central for supplementary material.

Acknowledgments

This work was support by grants from the National Science Foundation Plant Genome Program (DBI-0217653) to GRC and JCC, and the University of Nevada Agricultural Experiment Station, publication No. 03087111. Support for the Nevada Proteomics Center was made possible by NIH Grant Number P20 RR-016464 from the INBRE-BRIN Program of the National Center for Research Resources and the NIH IDeA Network of Biomedical Research Excellence (INBRE, RR-03-008). The authors thank Kathy Schegg and David Quilici of the Nevada Proteomics Center for support and for performing MS analyses and Rebecca Albion and Kitty Spreeman for invaluable technical support. The authors would like to especially thank Leon Sobon of Sobon Estate and Shenandoah Vineyards, Amador County, California (http://www.sobonwine.com/) for allowing us to collect the berry samples used in this study.

Abbreviations

CA	carrier ampholyte
MSTFA	N-Methyl-N-trimethylsilyltrifluoroacetamide
PR	pathogenesis-related
PMSF	phenylmethanesulphonylfluoride
PVPP	polyvinylpyrrolidone
RuBisCO	ribulose 1,5-bisphosphate carboxylase/oxygenase
TMCS	Trimethylchlorosilane

References

1. This P, Lacombe T, Thomas M. Historical origins and genetic diversity of wine grapes. Trends Genet. 2006; 22:511–519. [PubMed: 16872714]
2. Arroyo-Garcia R, Ruiz-Garcia L, Bolling L, Ocete R, et al. Multiple origins of cultivated grapevine (Vitis vinifera L. ssp. sativa) based on chloroplast DNA polymorphisms. Molec. Ecol. 2006; 15:3707–3714. [PubMed: 17032268]
3. Iriti M, Faoro F. Grape phytochemicals: a bouquet of old and new nutraceuticals for human health. Medical Hypotheses. 2006; 67:833–838. [PubMed: 16759816]
4. Monagas M, Hernandez-Ledesma B, Gomez-Cordoves C, Bartolome B. Commercial dietary ingredients from Vitis vinifera L. leaves and grape skins: antioxidant and chemical characterization J. Agric. Food Chem. 2006; 54:319–327.
5. This P, Lacombe T, Cadle-Davidson M, Owens C. Wine grape (Vitis vinifera L.) color associates with allelic variation in the domestication gene VvmybA1. Theor. Appl. Genet. 2007; 114:723–730. [PubMed: 17221259]
6. Bogs J, Jaffe F, Takos A, Walker A, Robinson S. The grapevine transcription factor VvMYBPA1 regulates proanthocyanidin synthesis during fruit development. Plant Physiol. 2007; 143:1347–1361. [PubMed: 17208963]
7. Fernandez K, Kennedy J, Agosin E. Characterization of Vitis vinifera L. Cv. Carmenere grape and wine proanthocyanidins. J. Agric. Food Chem. 2007; 55:3675–3680. [PubMed: 17407309]

8. Lund S, Bohlmann J. The molecular basis for wine grape quality--a volatile subject. Science. 2006; 311:804–805. [PubMed: 16469915]
9. Moreno-Arribas M, Cabello F, Polo M, Martin-Alvarez P, Pueyo E. Assessment of the native electrophoretic analysis of total grape must proteins for the characterization of Vitis vinifera L. cultivars. J. Agric. Food Chem. 1999; 47:114–120. [PubMed: 10563858]
10. Hayasaka Y, Adams K, Pocock K, Baldock G, et al. Use of electrospray mass spectrometry for mass determination of grape (Vitis vinifera) juice pathogenesis-related proteins: a potential tool for varietal differentiation. J. Agric. Food Chem. 2001; 49:1830–1839. [PubMed: 11308333]
11. Monteiro S, Picarra-Pereira M, Teixeira A, Loureiro V, Ferreira R. Environmental conditions during vegetative growth determine the major proteins that accumulate in mature grapes. J. Agric. Food Chem. 2003; 51:4046–4053. [PubMed: 12822945]
12. Vincent D, Wheatley M, Cramer G. Optimization of protein extraction and solubilization for mature grape berry clusters. Electrophoresis. 2006; 27:1853–1865. [PubMed: 16586412]
13. Sarry J-E, Sommerer N, Sauvage F-X, Bergoin A, et al. Grape berry biochemistry revisited upon proteomic analysis of the mesocarp. Proteomics. 2004; 4:201–215. [PubMed: 14730682]
14. Carvalho L, Esquivel M, Martins I, Ricardo C, Amancio S. Monitoring the stability of Rubisco in micropropagated grapevine (Vitis vinifera L.) by two-dimensional electrophoresis. J. Plant Physiol. 2005; 162:365–374. [PubMed: 15900878]
15. Castro A, Carapito C, Zorn N, Magne C, et al. Proteomic analysis of grapevine (Vitis vinifera L.) tissues subjected to herbicide stress. J. Exp. Bot. 2005; 56:2783–2795. [PubMed: 16216849]
16. Vincent D, Ergul A, Bohlman M, Tattersall E, et al. Proteomic analysis reveals differences between Vitis vinifera L. cv. Chardonnay and cv. Cabernet Sauvignon and their responses to water deficit and salinity. J. Exp. Bot. 2007; 58:1873–1892. [PubMed: 17443017]
17. Sauvage F-X, Pradal M, Chatelet P, Tesniere C. Proteome changes in leaves from grapevine (Vitis vinifera L.) transformed for alcohol dehydrogenase activity. J. Agric. Food Chem. 2007; 55:2597–2603. [PubMed: 17348683]
18. Deytieux C, Geny L, Lapaillerie D, Claverol S, et al. Proteome analysis of grape skins during ripening. J. Exp. Bot. 2007; 58:851–1862.
19. Giribaldi M, Perugini I, Sauvage F, Schubert A. Analysis of protein changes during grape berry ripening by 2-DE and MALDI-TOF. Proteomics. 2007; 7:3154–3170. [PubMed: 17683049]
20. Negri A, Prinsi B, Rossoni M, Failla O, et al. Proteome changes in the skin of the grape cultivar Barbara among different stages of ripening. BMC Genomics. 2008; 9:378. [PubMed: 18691399]
21. Moser C, Segala C, Fontana P, Salakhudtinov I, et al. Comparative analysis of expressed sequence tags from different organs of Vitis vinifera L. Funct. Integ. Genomics. 2005; 5:208–217.
22. da Silva F, Iandolino A, Al-Kayal F, Bohlmann M, et al. Characterizing the grape transcriptome. Analysis of expressed sequence tags from multiple Vitis species and development of a compendium of gene expression during berry development. Plant Physiol. 2005; 139:574–597. [PubMed: 16219919]
23. Peng F, Reid K, Liao N, Schlosser J, et al. Generation of ESTs in Vitis vinifera wine grape (Cabernet Sauvignon) and table grape (Muscat Hamburg) and discovery of new candidate genes with potential roles in berry development. Gene. 2007; 402:40–50. [PubMed: 17761391]
24. Waters L, Holton T, Ablett E, Lee L, Henry R. cDNA microarrays analysis of developing grape (Vitis vinifera cv. Shiraz) berry skin. Funct. Integ. Genomics. 2005; 5:40–58.
25. Terrier N, Glissant D, Grimplet J, Barrieu F, et al. Isogene specific oligo arrays reveal multifaceted changes in gene expression during grape berry (Vitis vinifera L.) development. Planta. 2005; 222:832–847. [PubMed: 16151847]
26. Pilati S, Perazzolli M, Malossini A, Cestaro A, et al. Genome-wide transcriptional analysis of grapevine berry ripening reveals a set of genes similarly modulated during three seasons and the occurrence of an oxidative burst at vèraison. BMC Genomics. 2007; 8:428. [PubMed: 18034875]
27. Deluc L, Grimplet J, Wheatley M, Tillett R, et al. Transcriptomic and metabolite analyses of Cabernet Sauvignon grape berry development. BMC Genomics. 2007; 8:429. [PubMed: 18034876]

28. Fernandez L, Torregrosa L, Terrier N, Sreekantan L, et al. Identification of genes associated with flesh morphogenesis during grapevine fruit development. Plant Molec. Biol. 2007; 63:307–323. [PubMed: 17268889]
29. Waters D, Holton T, Ablett E, Slade L, Henry R. The ripening wine grape berry skin transcriptome. Plant Sci. 2006; 171:132–138.
30. Grimplet J, Deluc L, Tillett R, Wheatley M, et al. Tissue-specific mRNA expression profiling in grape berry tissues. BMC Genomics. 2007; 8:187. [PubMed: 17584945]
31. Coombe B. Adoption of a system for identifying grapevine growth stages. Aust. J. Grape. Wine. Res. 1995; 1:104–110.
32. McCutchan J, Shackel K. Stem-water potential as a sensitive indicator of water stress in prune trees (Prunus domestica L. cv. French). J. Amer. Soc. Hort. Sci. 1992; 117:607–611.
33. Saravanan R, Rose J. A critical evaluation of sample extraction techniques for enhanced proteomic analysis of recalcitrant plant tissues. Proteomics. 2004; 4:2522–2532. [PubMed: 15352226]
34. Hurkman W, Tanaka C. Solubilization of plant membrane proteins for analysis bytwo-dimensional gel electrophoresis. Plant Physiol. 1986; 81:802–806. [PubMed: 16664906]
35. O'Farrell P. High resolution two-dimensional electrophoresis of proteins. J. Biol. Chem. 1975; 250:4007–4021. [PubMed: 236308]
36. Neuhoff V, Arold N, Taube D, Ehrhardt W. Improved staining of proteins in polyacrylamide gels including isoelectric focusing gels with clear background at nanogram sensitivity using Coomassie Brilliant Blue G-250 and R-250. Electrophoresis. 1988; 9:255–262. [PubMed: 2466658]
37. Rosenfeld J, Capdevielle J, Guillemot J, Ferrara P. In-gel digestion of proteins for internal sequence analysis after one- or two-dimensional gel electrophoresis. Anal. Biochem. 1992; 203:173–179. [PubMed: 1524213]
38. Zhu X, Papayannopoulos I. Improvement in the detection of low concentration protein digests on a MALDI TOF/TOF workstation by reducing alpha-cyano-4-hydroxycinnamic acid adductions. J. Biomolec.Techniq. 2003; 14:298–307.
39. Didier G, Brezellec P, Remy E, Henaut A. GeneANOVA-gene expression analysis of variance. Bioinform. 2002; 18:490–491.
40. Broeckling C, Huhman D, Farag M, Smith J, et al. Metabolic profiling of Medicago truncatula cell cultures reveals the effects of biotic and abiotic elicitors on metabolism. J. Exp. Bot. 2005; 56:323–336. [PubMed: 15596476]
41. Kopka J, Schauer N, Krueger S, Birkemeyer C, et al. GMD@CSB.DB: the Golm Metabolome Database. Bioinform. 2005; 21:1635–1638.
42. Chone X, Van Leeuwen C, Dubourdieu D, Gaudillere J. Stem water potential is a sensitive indicator of grapevine water status. Ann. Bot. (Lond). 2001; 87:477–483.
43. Parker R, Flowers T, Moore A, Harpham N. An accurate and reproducible method for proteome profiling of the effects of salt stress in the rice leaf lamina. J. Exp. Bot. 2006; 57:1109–1118. [PubMed: 16513811]
44. Hajduch M, Casteel J, Hurrelmeyer K, Song Z, et al. Proteomic analysis of seed filling in Brassica napus. Developmental characterization of metabolic isozymes using high-resolution two-dimensional gel electrophoresis. Plant Physiol. 2006; 141:32–46. [PubMed: 16543413]
45. Asirvatham V, Watson B, Sumner L. Analytical and biological variances associated with proteomic studies of Medicago truncatula by two-dimensional polyacrylamide gel electrophoresis. Proteomics. 2002; 2:960–968. [PubMed: 12203891]
46. Grimplet, J.; Deluc, L.; Cramer, G.; Cushman, J.; Matthew, A.; Jenks, PMH.; Jain, SM., editors. Advances in molecular-breeding toward drought and salt tolerant crops. Springer; Dordrecht, The Netherlands: 2007.
47. Escalona J, Flexas J, Bota J, Medrano H. Distribution of leaf photosynthesis and transpiration within grapevine canopies under different drought conditions. Vitis. 2003; 42:57–64.
48. Ageorges A, Fernandez L, Vialet S, Merdinoglu D, et al. Four specific isogenes of the anthocyanin metabolic pathway are systematically co-expressed with the red colour of grape berries. Plant Sci. 2006; 170:372–383.
49. Shi J, Yu J, Pohorly J, Kakuda Y. Polyphenolics in grape seeds-biochemistry and functionality. J. Medic. Food. 2003; 6:291–299.

50. Ibdah M, Zhang X, Schmidt J, Vogt T. A novel Mg(2+)-dependent O-methyltransferase in the phenylpropanoid metabolism of Mesembryanthemum crystallinum. J. Biol. Chem. 2003; 278:43961–43972. [PubMed: 12941960]
51. Castellarin S, Di Gaspero G, Marconi R, Nonis A, et al. Colour variation in red grapevines (Vitis vinifera L.): genomic organisation, expression of flavonoid 3′-hydroxylase, flavonoid 3′,5′-hydroxylase genes and related metabolite profiling of red cyanidin-/blue delphinidin-based anthocyanins in berry skin. BMC Genomics. 2006; 7:12. [PubMed: 16433923]
52. Kobayashi S, Ishimaru M, Hiraoka K, Honda C. Myb-related genes of the Kyoho grape (Vitis labruscana) regulate anthocyanin biosynthesis. Planta. 2002; 215:924–933. [PubMed: 12355152]
53. Kobayashi S, Goto-Yamamoto N, Hirochika H. Retrotransposon-induced mutations in grape skin color. Science. 2004; 304:982. [PubMed: 15143274]
54. Ford C, Boss P, Hoj P. Cloning and characterization of Vitis vinifera UDP-glucose:flavonoid 3-O-glucosyltransferase, a homologue of the enzyme encoded by the maize Bronze-1 locus that may primarily serve to glucosylate anthocyanidins in vivo. J. Biol. Chem. 1998; 273:9224–9233. [PubMed: 9535914]
55. Alfenito M, Souer E, Goodman C, Buell R, et al. Functional complementation of anthocyanin sequestration in the vacuole by widely divergent glutathione S-transferases. Plant Cell. 1998; 10:1135–1149. [PubMed: 9668133]
56. Kobayashi S, Ishimaru M, Ding C, Yakushiji H, Goto N. Comparison of UDP-glucose:flavonoid 3-O-glucosyltransferase (UFGT) gene sequences between white grapes (Vitis vinifera) and their sports with red skin. Plant Sci. 2001; 160:543–550. [PubMed: 11166442]
57. Wang X, He X, Lin J, Shao H, et al. Crystal structure of isoflavone reductase from Alfalfa (Medicago sativa L.). J. Molec. Biol. 2006; 358:1341–1352. [PubMed: 16600295]
58. Famiani F, Walker R, Tecsi L, Chen Z, et al. An immunohistochemical study of the compartmentation of metabolism during the development of grape (Vitis vinifera L.) berries. J. Exp. Bot. 2000; 51:675–683. [PubMed: 10938859]
59. Edwards J, Walker E, Coruzzi G. Cell-specific expression in transgenic plants reveals nonoverlapping roles for chloroplast and cytosolic glutamine synthetase. Proc. Natl. Acad. Sci. USA. 1990; 87:3459–3463. [PubMed: 1970638]
60. Pripis-Nicolau L, de Revel G, Bertrand A, Lonvaud-Funel A. Methionine catabolism and production of volatile sulphur compounds by Oenococcus oeni. J. Appl. Microbiol. 2004; 96:1176–1184. [PubMed: 15078536]
61. Hernandez-Orte P, Cacho J, Ferreira V. Relationship between varietal amino acid profile of grapes and wine aromatic composition. Experiments with model solutions and chemometric study. J. Agric. Food Chem. 2002; 50:2891–2899. [PubMed: 11982416]
62. Hashizume K, Tozawa K, Endo M, Aramaki I. S-Adenosyl-L-methionine-dependent O-methylation of 2-hydroxy-3-alkylpyrazine in wine grapes: a putative final step of methoxypyrazine biosynthesis. Biosci. Biotechnol. Biochem. 2001; 65:795–801.
63. Stines A, Naylor D, Hoj P, van Heeswijck R. Proline accumulation in developing grapevine fruit occurs independently of changes in the levels of delta1-pyrroline-5-carboxylate synthetase mRNA or protein. Plant Physiol. 1999; 120:923–931. [PubMed: 10398729]
64. Ibarz M, Ferreira V, Hernández-Orte P, Loscos N, Cacho J. Optimization and evaluation of a procedure for the gas chromatographic-mass spectrometric analysis of the aromas generated by fast acid hydrolysis of flavor precursors extracted from grapes. J. Chromatogr. A. 2006; 1116:217–229. [PubMed: 16581079]
65. Rojas-Beltran J, Dubois F, Mortiaux F, Portetelle D, et al. Identification of cytosolic Mg2+-dependent soluble inorganic pyrophosphatases in potato and phylogenetic analysis. Plant Mol. Biol. 1999; 39:449–461. [PubMed: 10092174]
66. Davies C, Robinson S. Differential screening indicates a dramatic change in mRNA profiles during grape berry ripening. Cloning and characterization of cDNAs encoding putative cell wall and stress response proteins. Plant Physiol. 2000; 122:803–812. [PubMed: 10712544]
67. Tamburrini M, Cerasuolo I, Carratore V, Stanziola A, et al. Kiwellin, a novel protein from kiwi fruit. Purification, biochemical characterization and identification as an allergen. Protein J. 2005; 24:423–429. [PubMed: 16328735]

68. Fahlbusch B, Rudeschko O, Schumann C, Steurich F, et al. Further characterization of IgE-binding antigens in kiwi, with particular emphasis on glycoprotein allergens. J. Investig. Allergol. Clin. Immunol. 1998; 8:325–332.
69. Huby R, Dearman R, Kimber I. Why are some proteins allergens? Toxicol Sci. 2000; 55:235–246. [PubMed: 10828254]
70. Reuter A, Fortunato D, Garoffo L, Napolitano L, et al. Novel isoforms of Pru av 1 with diverging immunoglobulin E binding properties identified by a synergistic combination of molecular biology and proteomics. Proteomics. 2005; 5:282–289. [PubMed: 15593144]
71. Caporale C, Facchiano A, Bertini L, Leonardi L, et al. Comparing the modeled structures of PR-4 proteins from wheat. J. Mol. Model. 2003; 9:9–15. [PubMed: 12638007]
72. Aziz A, Heyraud A, Lambert B. Oligogalacturonide signal transduction, induction of defense-related responses and protection of grapevine against Botrytis cinerea. Planta. 2004; 218:767–774. [PubMed: 14618326]
73. Wimmer B, Lottspeich F, van der Klei I, Veenhuis M, Gietl C. The glyoxysomal and plastid molecular chaperones (70-kDa heat shock protein) of watermelon cotyledons are encoded by a single gene. Proc. Natl. Acad. Sci. USA. 1997; 94:13624–13629. [PubMed: 9391076]
74. Liu Y, Burch-Smith T, Schiff M, Feng S, Dinesh-Kumar S. Molecular chaperone Hsp90 associates with resistance protein N and its signaling proteins SGT1 and Rar1 to modulate an innate immune response in plants. J. Biol. Chem. 2004; 279:2101–2108. [PubMed: 14583611]
75. Boulton, R.; Singleton, V.; Bisson, L.; Kunkee, R. Principles and Practices of Winemaking Aspen Publishers. New York: 1998.
76. Dry I, Robinson S. Molecular cloning and characterisation of grape berry polyphenol oxidase. Plant Mol. Biol. 1994; 26:495–502. [PubMed: 7948897]
77. Rathjen H, Robinson S. Characterisation of a variegated grapevine mutant ahowing reduced polyphenol oxidase activity. Funct. Plant Biol. 1992; 19:43–54.
78. Battaglia M, Olvera-Carrillo Y, Garciarrubio A, Campos F, Covarrubias A. The enigmatic LEA proteins and other hydrophilins. Plant Physiol. 2008; 148:6–24. [PubMed: 18772351]
79. Soulages J, Kim K, Arrese E, Walters C, Cushman J. Conformation of a group 2 late embryogenesis abundant protein from soybean. Evidence of poly (L-proline)-type II structure. Plant Physiol. 2003; 131:963–975. [PubMed: 12644649]
80. DeBolt S, Cook D, Ford C. L-tartaric acid synthesis from vitamin C in higher plants. Proc. Natl. Acad. Sci. USA. 2006; 103:5608–5613. [PubMed: 16567629]
81. Possner D, Kliewer W. The localization of acids, sugars, potassium and calcium in developing grape berries. Vitis. 1985; 24:229–240.
82. Debolt S, Melino V, Ford C. Ascorbate as a biosynthetic precursor in plants. Ann. Bot. (Lond). 2007; 99:3–8.
83. Mato I, Suarez-Luque S, Huidobro J. Simple determination of main organic acids in grape juice and wine by using capillary zone electrophoresis with direct UV detection. Food Chem. 2007; 102:104–112.
84. Conde C, Agasse A, Glissant D, Tavares R, et al. Pathways of glucose regulation of monosaccharide transport in grape cells. Plant Physiol. 2006; 141:1563–1577. [PubMed: 16766675]
85. Hawker JS, Ruffner H, Walker R. The sucrose content of some australian grapes. Amer. J. Enol. Vitic. 1976; 27:125–129.
86. Garlick A, Moore C, Kruger N. Monitoring flux through the oxidative pentose phosphate pathway using [1-14C]gluconate. Planta. 2002; 216:265–272. [PubMed: 12447540]
87. Peinado R, Moreno J, Medina M, Mauricio J. Potential application of a glucose-transport-deficient mutant of Schizosaccharomyces pombe for removing gluconic acid from grape must. J. Agric. Food Chem. 2005; 53:1017–1021. [PubMed: 15713014]
88. Gomez L, Baud S, Graham I. The role of trehalose-6-phosphate synthase in Arabidopsis embryo development. Biochem. Soc. Trans. 2005; 33:280–282. [PubMed: 15667326]
89. D'Arcy-Lameta A, Ferrari-Iliou R, Contour-Ansel D, Pham-Thi A, Zuily-Fodil Y. Isolation and characterization of four ascorbate peroxidase cDNAs responsive to water deficit in cowpea leaves. Ann. Bot. (Lond). 2006; 97:133–140.

90. Castellarin S, Pfeiffer A, Sivilotti P, Degan M, et al. Transcriptional regulation of anthocyanin biosynthesis in ripening fruits of grapevine under seasonal water deficit. Plant Cell. Environ. 2007; 30:1381–1399. [PubMed: 17897409]
91. Castellarin S, Matthews M, Di Gaspero G, Gambetta G. Water deficits accelerate ripening and induce changes in gene expression regulating flavonoid biosynthesis in grape berries. Planta. 2007; 227:101–112. [PubMed: 17694320]
92. Fait A, Fromm H, Walter D, Galili G, Fernie A. Highway or byway: the metabolic role of the GABA shunt in plants. Trends Plant Sci. 2007; 13:14–19. [PubMed: 18155636]
93. Bytof G, Knopp S-E, Schieberle P, Teutsch I, Selmar D. Influence of processing on the generation of gamma-aminobutyric acid in green coffee beans. Euro. Food Res. Tech. 2005; 220:245–250.
94. Rhodes D, Handa S, Bressan R. Metabolic changes associated with adaptation of plant cells to water stress. Plant Physiol. 1986; 82:890–903. [PubMed: 16665163]
95. Taji T, Ohsumi C, Iuchi S, Seki M, et al. Important roles of drought- and cold-inducible genes for galactinol synthase in stress tolerance in Arabidopsis thaliana. Plant J. 2002; 29:417–426. [PubMed: 11846875]
96. Robinson S, Jacobs A, Dry I. A class IV chitinase is highly expressed in grape berries during ripening. Plant Physiol. 1997; 114:771–778. [PubMed: 9232868]
97. Tesnière C, Torregrosa L, Pradal M, Souquet J, et al. Effects of genetic manipulation of alcohol dehydrogenase levels on the response to stress and the synthesis of secondary metabolites in grapevine leaves. J. Exp. Bot. 2006; 57:91–99. [PubMed: 16291801]
98. Coleman H, Ellis D, Gilbert M, Mansfield S. Up-regulation of sucrose synthase and UDP-glucose pyrophosphorylase impacts plant growth and metabolism. Plant Biotechnol. J. 2006; 4:87–101. [PubMed: 17177788]
99. Watson B, Asirvatham V, Wang L, Sumner W. Mapping the proteome of barrel medic (Medicago truncatula). Plant Physiol. 2003; 131:1104–1123. [PubMed: 12644662]
100. Liu Y, Lamkemeyer T, Jakob A, Mi G, et al. Comparative proteome analyses of maize (Zea mays L.) primary roots prior to lateral root initiation reveal differential protein expression in the lateral root initiation mutant rum1. Proteomics. 2006; 6:4300–4308. [PubMed: 16819721]
101. Faurobert M, Mihr C, Bertin N, Pawlowski T, et al. Major proteome variations associated with cherry tomato pericarp development and ripening. Plant Physiol. 2007; 143:1327–1346. [PubMed: 17208958]
102. Gion J-M, Lalanne C, Le Provost G, Ferry-Dumazet H, et al. The proteome of maritime pine wood forming tissue. Proteomics. 2005; 5:3731–3751. [PubMed: 16127725]

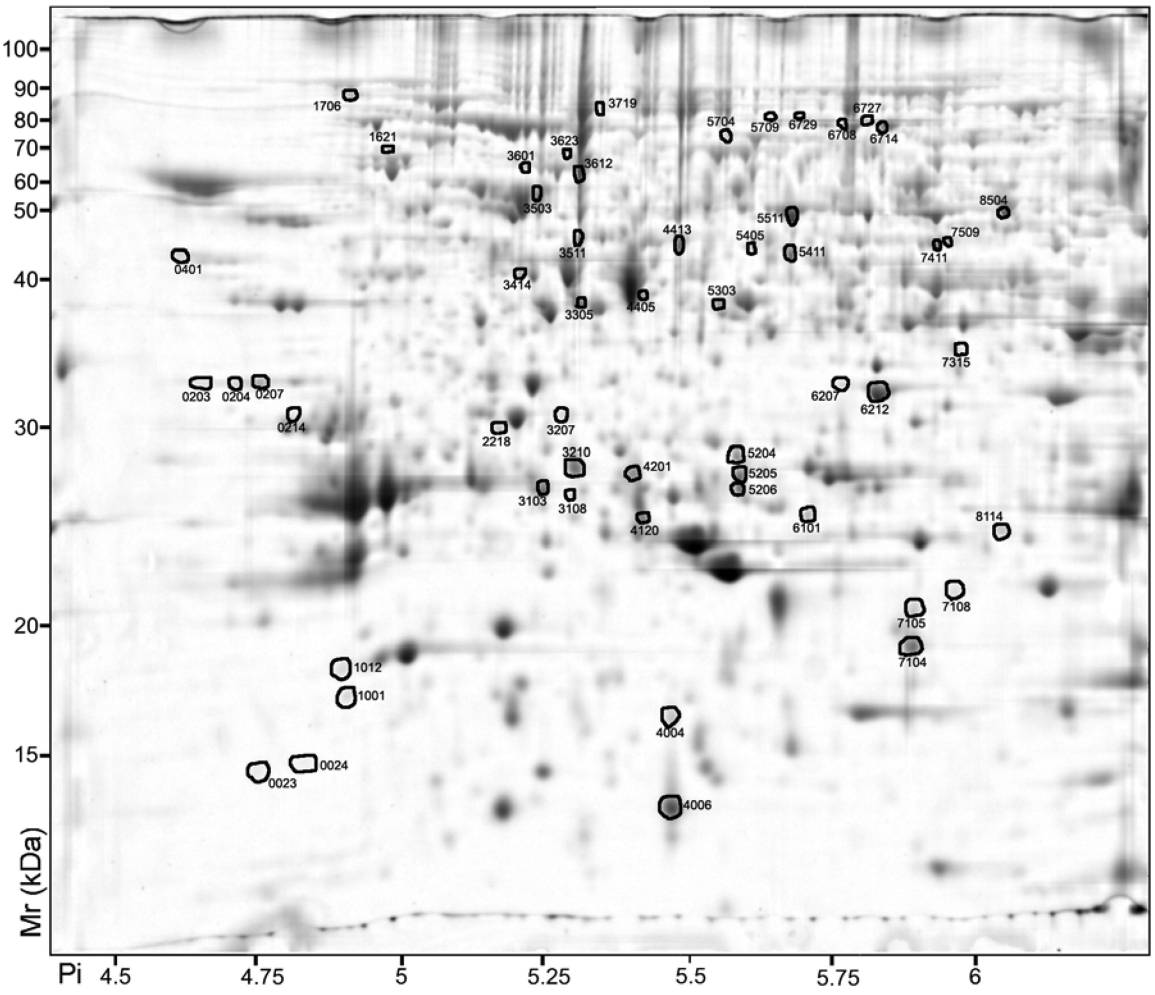

Figure 1.

2D-PAGE analysis of *Vitis vinifera* cv. Cabernet Sauvignon berry skin proteins. Proteins that exhibited a significant ($p < 0.05$) two-fold or greater change between the skin and pulp are indicated by circles and standard spot numbers on a representative gel. See Table 3 for detailed listing of proteins.

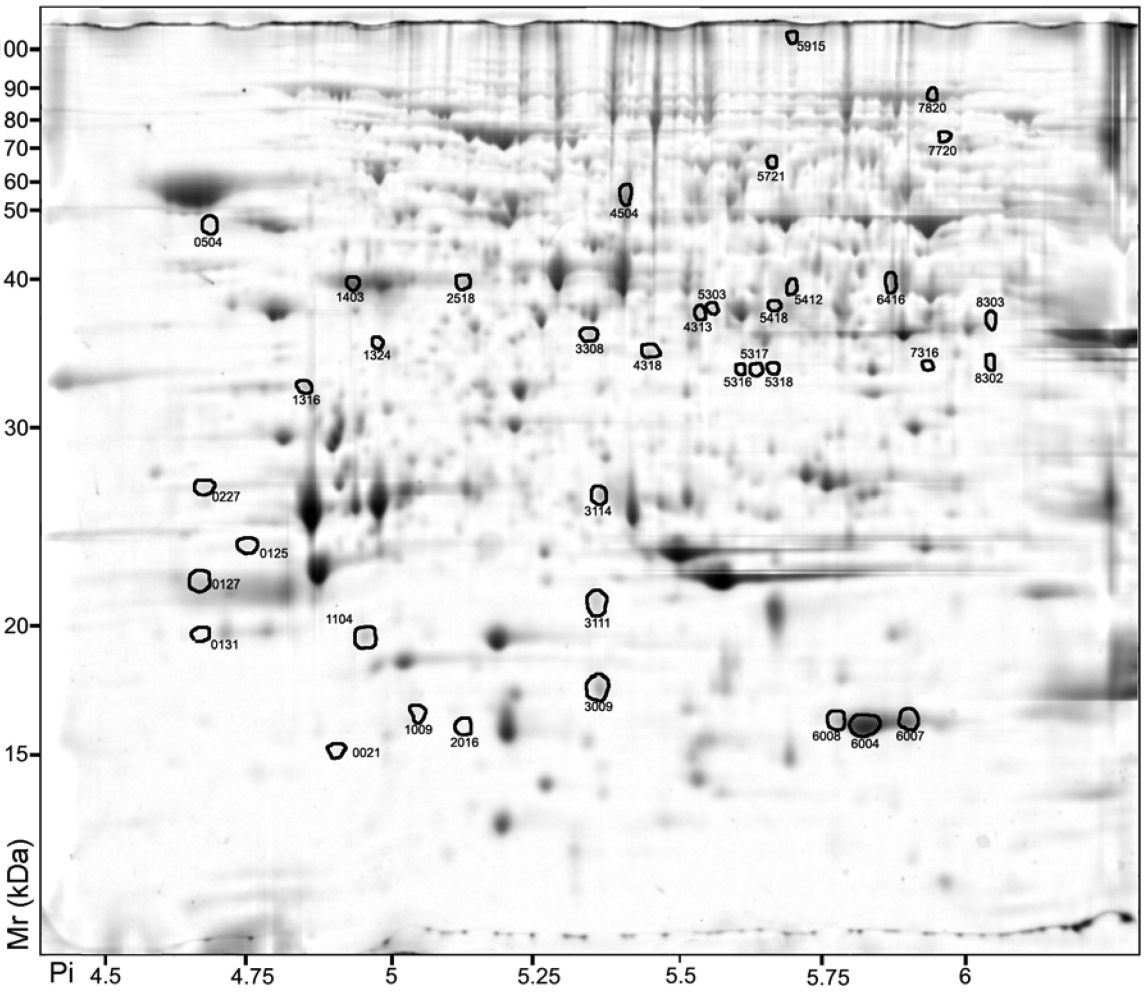

Figure 2.

2D-PAGE analysis of *Vitis vinifera* cv. Cabernet Sauvignon berry pulp proteins. Proteins that exhibited a significant ($p < 0.05$) two-fold or greater change between the skin and pulp are indicated by circles and standard spot numbers on a representative gel. See Table 3 for detailed listing of proteins.

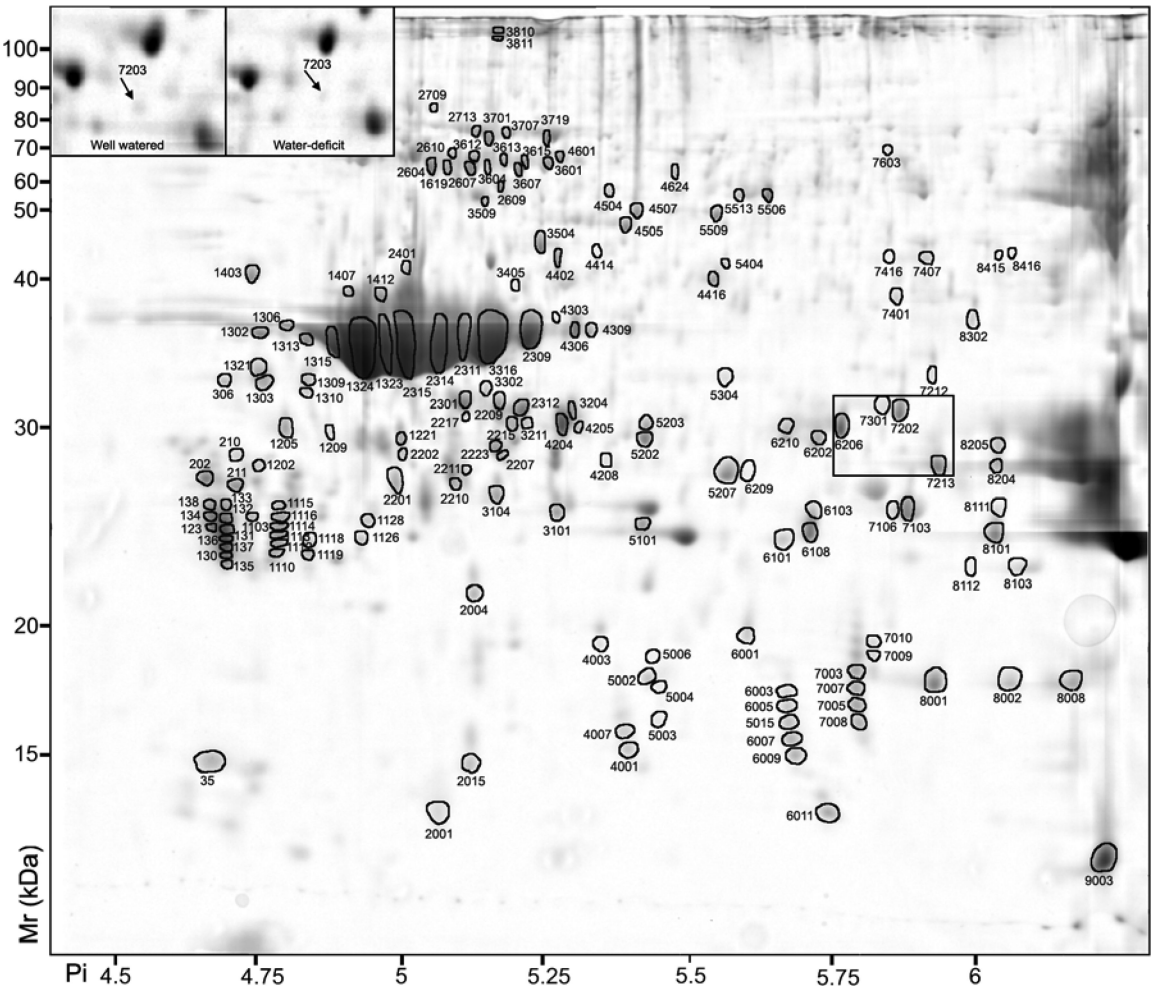

Figure 3.

2D-PAGE analysis of *Vitis vinifera* cv. Cabernet Sauvignon berry seed proteins. Proteins that exhibited a significant ($p < 0.05$) two-fold or greater change between the seed and pericarp tissues are indicated by circles and standard spot numbers on a representative gel. See Table 4 for detailed listing of proteins. Inset: spot 7203 (arrow), which was more abundant in seed of well watered than water-deficit treated berries.

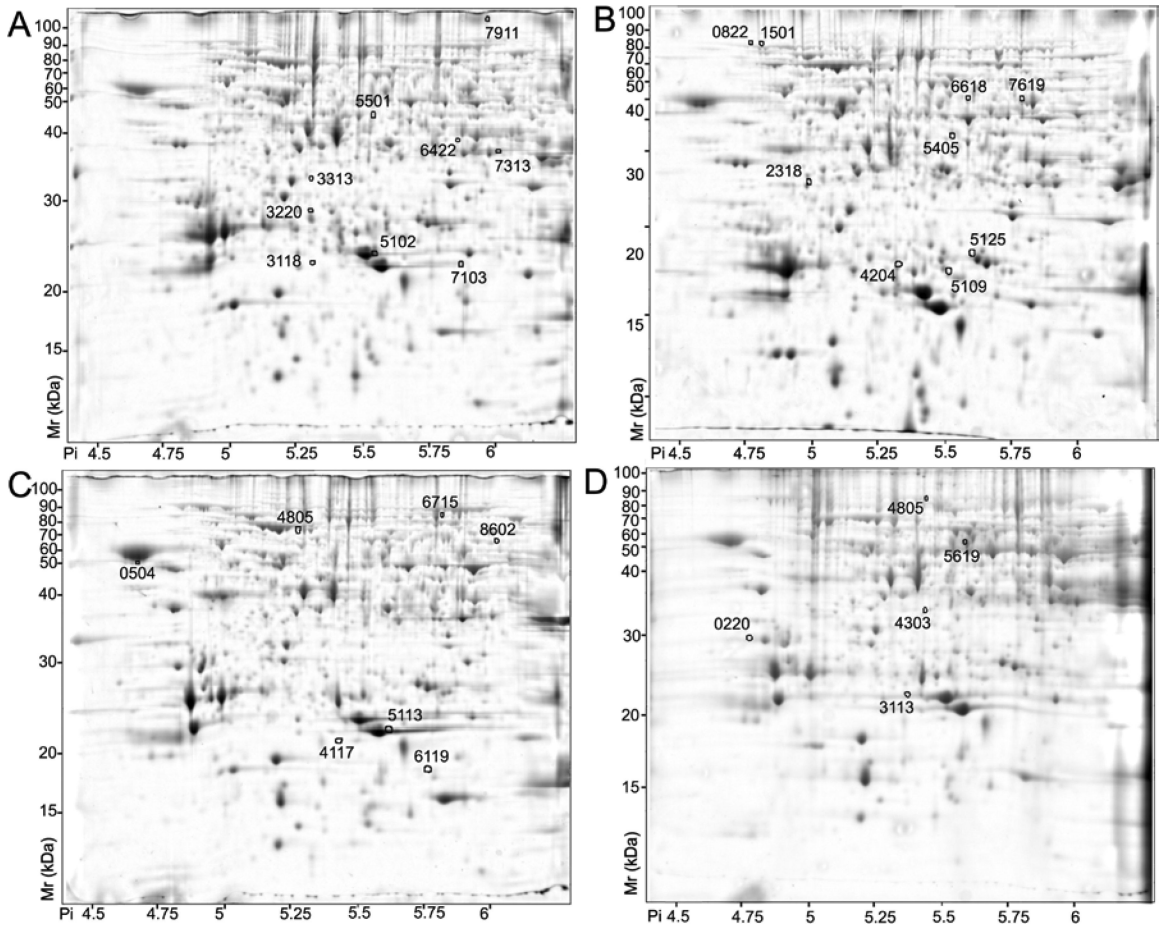

Figure 4.

Spots whose abundance differed significantly ($p < 0.05$; two-fold or greater change) with water status. A) Pulp proteins more abundant under well-watered conditions. B) Pulp proteins more abundant under water-deficit conditions. C) Skin proteins more abundant under well watered conditions. D) Skin proteins more abundant under water-deficit conditions are indicated by circles and standard spot numbers on a representative gel. See Tables 5 and 6 for detailed listing of pulp and skin proteins, respectively.

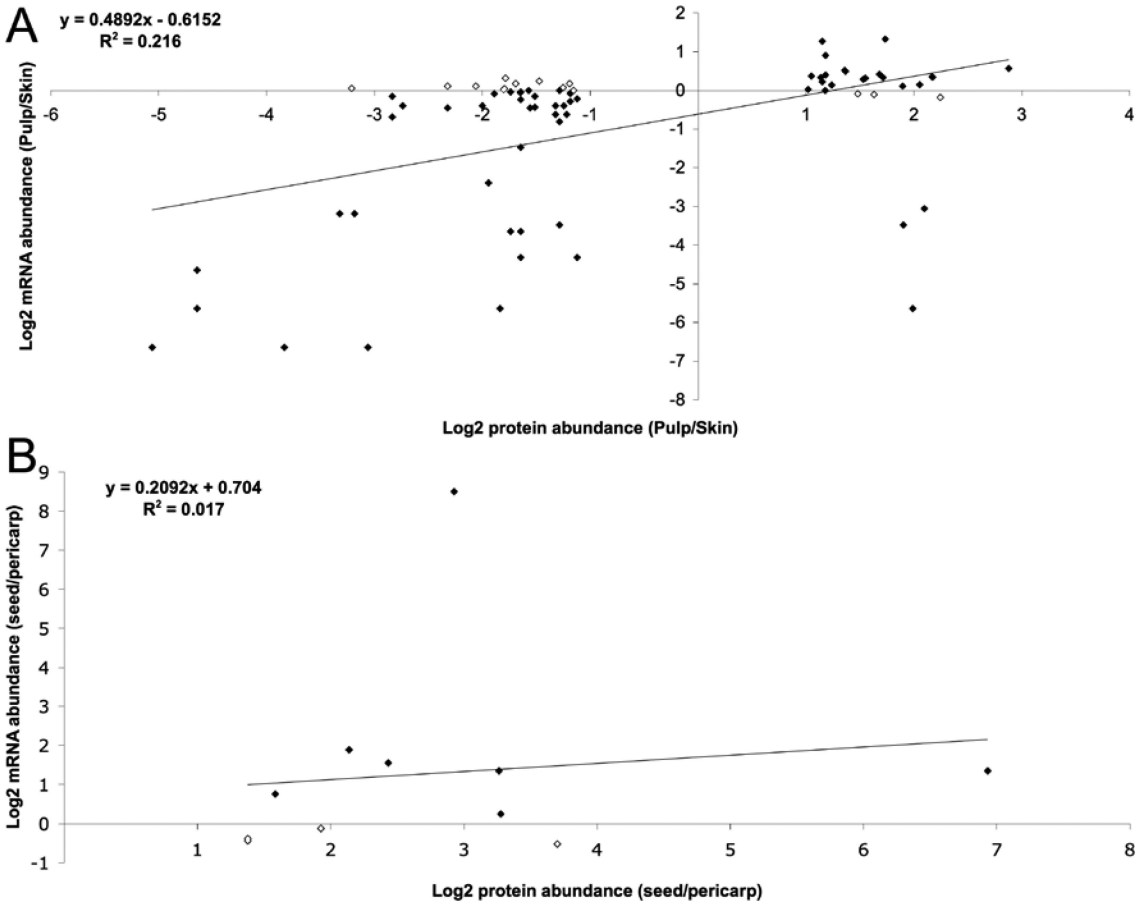

Figure 5.

Correlation of protein and mRNA abundance in different berry tissues. Values are expressed as $\log_2$ ratio of abundance: A) in pulp vs. skin B) in seed vs. pericarp. Solid diamonds represent individual gene products following similar trends for both mRNA and protein expression.

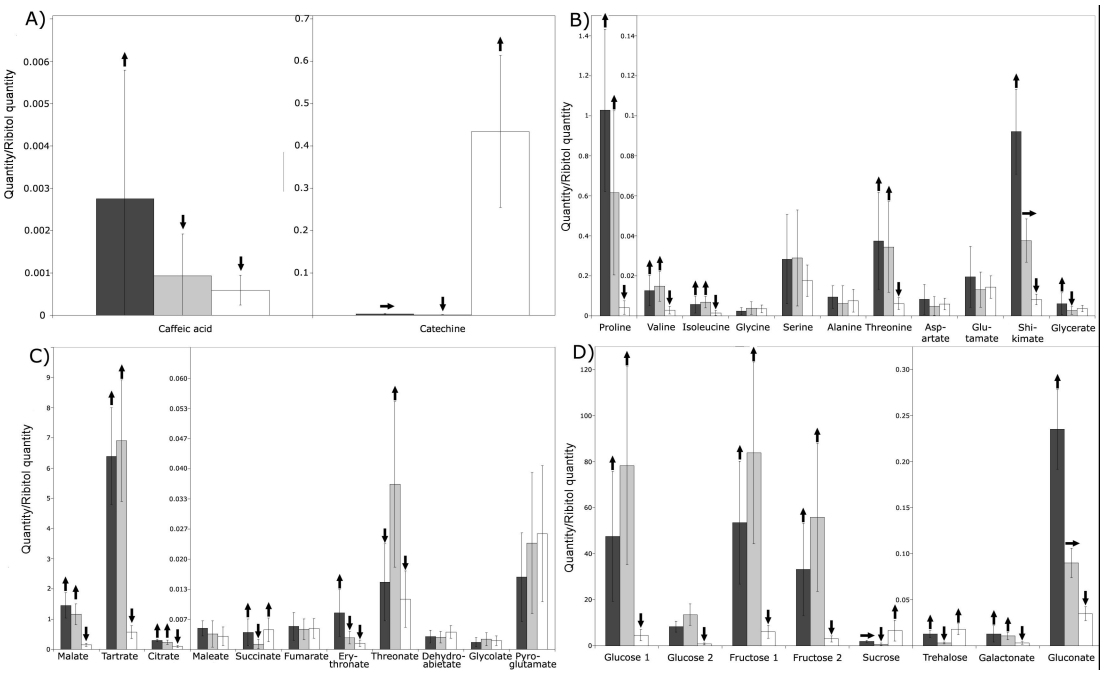

Figure 6.

Identification and quantitative differences of selected metabolites within different tissues: A) phenylpropanoids, B) amino acids, C) organics acids, and D) sugars. Skin (black bars), pulp (gray bars), seed (white bars). Up arrows indicate that the metabolite was significantly (ANOVA $p<0.005$, two-fold change or greater) more abundant than in tissues with a horizontal or arrow down. Horizontal arrows indicate that the metabolite was significantly ($p<0.005$, two-fold change or greater) less abundant than in tissues with an up arrow and more abundant than in tissues with a down arrow. Down arrows indicate that the metabolite was significantly ($p<0.005$, two-fold ratio change or greater) less abundant than in tissues with a horizontal or up arrow. Error bars represent standard deviation of the mean, n = 5.

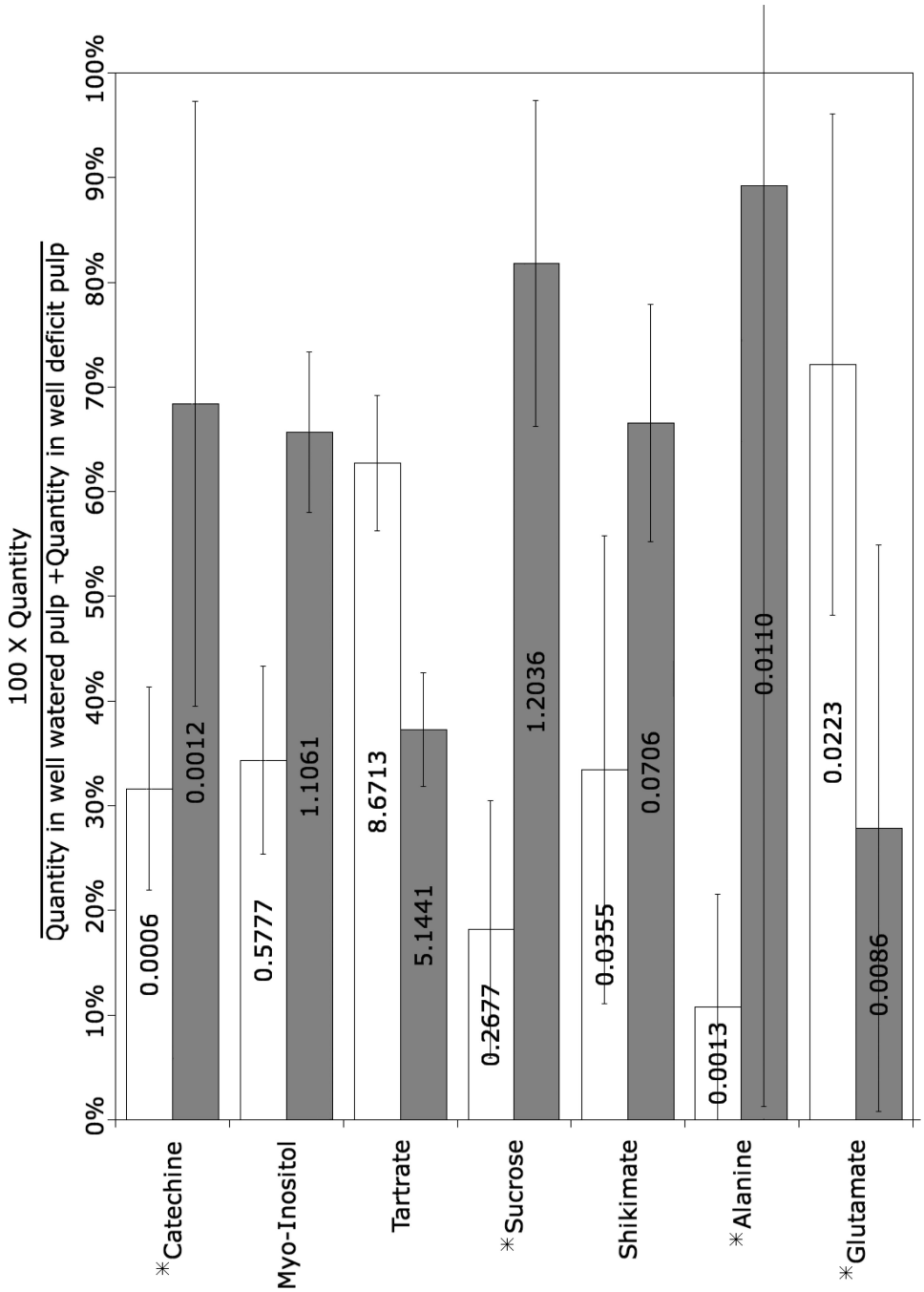

Figure 7.

Metabolites that differed significantly (ANOVA $p < 0.05$) between pulp derived from well watered and water-deficit treated vines. Asterisk (*) indicates metabolites that exhibited a two-fold or greater change in abundance. Error bars represent standard deviation of the mean, n = 5. Values within bars are the ratio relative to the internal standard (ribitol).

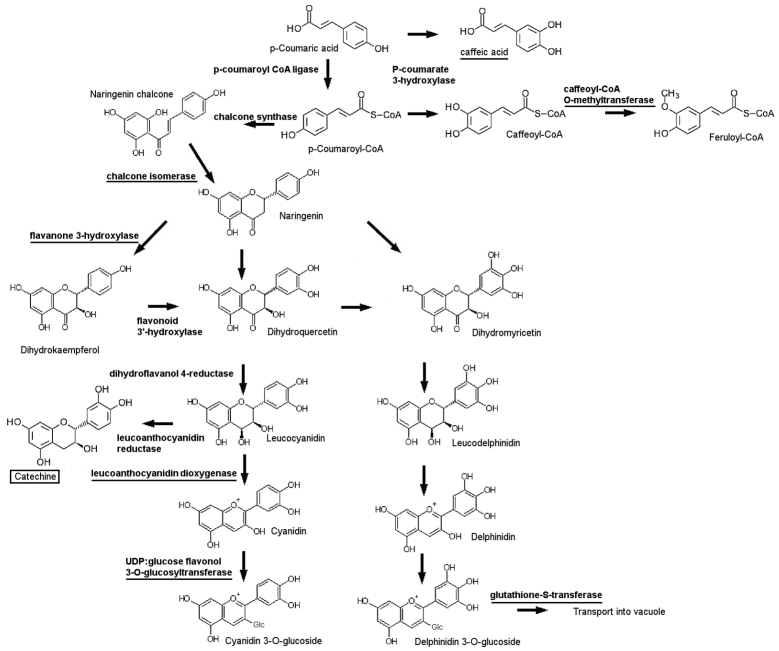

Figure 8. Enzymes and metabolites differentially expressed across tissues within a simplified flavonoid biosynthetic pathway

Underlined names indicate the enzymes or metabolites more abundant in skin; Boxed name indicates the metabolite more abundant in the seed.

Table 1

Physiological data for berries harvested from vines grown under well watered and water-deficit stress conditions.

Sample	Stem water potential (MPa)	Berry refractive index (°Brix)	Berry size (mm)
Well watered vine	−0.58 (±0.07)[a]	19.78 (±1.02)[a]	11.23 (±0.33)[a]
Water-deficit vine	−0.86 (±0.11)[a,b]	21.73 (±0.74)[a,b]	11.27 (±0.30)[a]

[a] n = 6.

[b] Difference between well watered and water-deficit were determined by to be significant (p-value < 0.01) by the student's t-test. Standard errors are indicated in parentheses.

Table 2

Average numbers of spots and coefficients of variation (CV) for each berry tissue and water treatment condition. The spots were counted regardless of their intensity (I) or according to CV values greater than 0.01% or 0.05% of the total intensity of all spots.

	SkinWW	SkinWD	PulpWW	PulpWD	SeedWW	SeedWD
Total spots	1046	1046	1046	1046	695	695
Average CV (total spots)	0.84	0.74	0.82	0.81	0.74	0.76
Spots (I>0.01%)	835±59	870±30	855±30	855±68	608±41	602±23
Average CV (I>0.01%)	0.65	0.58	0.64	0.63	0.59	0.60
Spots (I>0.05%)	462±55	509±20	457±37	482±48	365±109	366±58
Average CV (I>0.05%)	0.55	0.56	0.56	0.55	0.53	0.54

WW = well watered; WD = water-deficit treated. n = 6.

Table 3

Proteins whose abundance was significantly different between pulp and skin. SSP, standard spot number; P/K, normalized spot volume in the pulp divided by the normalized spot volume in the skin, from 12 different plants; Pval, P value; VvGI5, match from the translated *Vitis vinifera* gene index Release 5; ThMr, theoretical molecular mass; Exp Mr, experimental molecular mass; ThPi, theoretical isoelectric point (Pi); Exp Pi, experimental isoelectric point (Pi); Pep, number of peptides mass and number of MS/MS ions matching the query; Mowse score; % Cov, percentage of coverage; Annotation, description of protein identity; Uniprot, Uniprot ID of the most closely related Unigene from VvGI5.

SSP	P/K	Pval	VvGI5	ThMr	Exp Mr	ThPi	Exp Pi	Pep	Mowse score	% Cov	Annotation	Uniprot
Phenylpropanoid pathway												
6101	0.04	.000	TC69505	24222	24983	5.62	5.73	13+6	395	42	Glutathione S-transferase	Q56AY1 .
5411	0.04	.000	TC69652	40167	42968	5.63	5.70	35+6	539	75	Leucoanthocyanidin dioxgenase	Q8LP73
3103	0.10	.000	TC58036	25629	26375	5.37	5.26	7+2	129	12	Glutathione S-transferase	Q9M6R4
3210	0.11	.000	TC55034	26764	27699	5.61	5.31	9+4	313	30	Chalcone isomerase	P51117
5206	0.12	.000	TC70299	25341	26382	5.45	5.6	7+2	155	44	Caffeoyl-CoA O-methyltransferase	Q2YHM9
7411	0.28	.000	AF000371	50121	43883	5.98	5.96	13+5	335	28	UDP-glucose:flavonoid 3-O-glc transferase	Q9AR43
4405	0.32	.023	TC70298	40848	39433	5.44	5.44	17+7	526	41	Flavonone-3-hydroxylase	P41090
8302	3.33	.021	TC52848	33830	34548	6.16	6.05	6+4	220	18	Isoflavone reductase	O81355
Amino acid metabolism												
6714	0.30	.002	TC55403	77154	78904	6.04	5.86	12+2	84.3	31	Glycyl tRNA synthetase	O23627
4413	0.32	.000	TC51748	42930	42888	5.5	5.5	30+7	539	57	S-adenosylmethionine synthetase 2	Q96552
6708	0.32	.025	TC55403	77154	78220	6.04	5.79	8+2	167	22	Glycyl tRNA synthetase	O23627
5204	0.35	.002	TC58487	27173	28285	5.64	5.60	14+4	369	31	Aluminum-induced protein	Q9FG81
5303	0.41	.021	TC64127	41725	38816	5.7	5.57	17+7	213	31	Glutamine synthetase cytosolic isozyme 2	P51119
7509	0.41	.018	TC67021/TC51696	51280	44216	6.44	5.97	15+2/11+2	78.4/61.6	29/27	Ornithine aminotransferase/UDP-glucose:flavonoid 3-O-glc transferase	Q9FVJ2 /Q9AR43
3305	0.44	.003	TC60125	38931	38861	5.4	5.33	18+6	421	44	Glutamine synthetase	Q93XJ6
4318	4.15	.015	TC55907	35827	35829	5.24	5.48	9+2	65.8	31	Homocysteine S-methyltransferase	Q8LAX0
Energy												
1621	0.14	.000	TC67963	61983	67575	5.2	5.02	8+2	66.6	9	RuBisCO subunit binding-protein alpha	Q2PEP1
8504	0.20	.000	TC57584	52518	50702	6.33	6.08	30+8	398	21	RuBisCO, large subunit	Q9MVF6
203	0.25	.001	TC51789	24720	32916	4.6	4.66	12+2	101	37	Cytochrome c oxidase subunit 6b-1	Q8LHA3
4120	0.30	.007	TC62932	23416	24839	5.37	5.44	11+5	164	37	Chlorophyll a-b binding protein 8	P27522
3207	0.32	.000	TC54765	35289	30799	6.08	5.3	3+3	156	7	Oxygen evolving enhancer protein 1	Q9LRC4

SSP	P/K	Pval	VvGI5	ThMr	Exp Mr	ThPi	Exp Pi	Pep	Mowse score	% Cov	Annotation	Uniprot
204	0.33	.003	TC51789/TC52065	20911	32849	4.53	4.72	9+5/7+1	249/148	33/28	Cytochrome-c oxidase/Pru2 protein precursor	F86357 /Q43608
6729	0.40	.007	TC52655	50682	80938	6.47	5.72	20+4	174	31	Transketolase 1	O78327
2218	0.41	.006	TC53930	35091	29895	7.54	5.18	15+7	433	44	Oxygen evolving enhancer protein 1	Q9LRC4
6727	0.43	.011	TC52655	50682	80895	6.47	5.84	24+2	117	40	Transketolase 1	O78327
5511	0.44	.003	TC60581	47873	48953	5.67	5.70	25+8	896	51	Enolase 1	Q9LEJ0
3503	0.49	.015	TC63054[a]	59179	55592	5.9	5.25	9+3	124	41	ATP synthase beta chain, mitochondrial	P17614
3114	2.03	.012	TC56801	25524	26379	5.64	5.39	15+5	229	41	Soluble inorganic pyrophosphatase	Q6YVH9
8303	4.28	.006	TC52261	42948	36911	8.13	6.06	15+7	661	34	Plastidic fructose-bisphosphate aldolase	Q8LL68
Biotic and Abiotic Stress												
7104	0.03	.000	TC68949	17128	19044	5.96	5.92	8+3	189	24	Pathogenesis-related protein 10	Q9FS43
7105	0.07	.026	TC68949	17128	20473	5.96	5.92	7+6	223	24	Pathogenesis-related protein 10	Q9FS43
7108	0.27	.001	TC55027	22871	21286	4.71	5.99	2+2	143	7	Ripening-related protein grip22	Q9M4H4
1012	0.32	.046	TC51691	68396	18178	6.47	4.90	10+2	63.1	15	Polyphenol oxidase	P43311
1706	0.34	.000	TC54161	75365	78785	5.15	4.96	18+4	450	30	Heat shock protein 70	Q39641
4006	0.41	.000	TC58333	15716	13591	5.56	5.49	3+1	125	24	PR-4 type protein D	O81228
3719	0.44	.034	TC53932	47429	85072	5.11	5.36	4+3	88.7	8	Molecular chaperone Hsp90-1	Q6UJX6
6212	0.46	.037	TC61082	13359	32142	6.11	5.85	4+2	221	18	Beta 1-3 glucanase	Q9M3U4
1104	2.22	.023	TC52579	17262	19493	5.15	4.94	4+1	61.2	16	Peroxiredoxin	Q8S3L0
7720	2.27	.044	TC65221	65479	77910	6.04	5.99	18+0	47.4	31	Stress-induced protein sti1	Q9STH1
3111	2.79	.002	TC55027	22871	21329	4.71	5.36	3+3	86.9	11	Ripening-related protein grip22	Q9M4H4
2518	3.28	.005	TC68410	23681	41567	5.21	5.13	10+4	172	26	Dehydrin	Q41111
1009	3.97	.035	TC65039	17444	17639	4.97	5.05	2+2	165	12	Major cherry allergen Pru av1.0201	Q6QHU2
1403	4.49	.025	TC68410	23681	41193	5.21	4.93	18+6	397	34	Dehydrin	Q41111
Other metabolism												
5405	0.20	.002	TC59251	15662	43636	5.48	5.63	4+3	66	23	GDP-mannose pyrophosphorylase	Q8W4J5
7315	0.24	.022	TC55889	34731	35180	6.07	6	8+2	63.3	19	NADPH-dependent mannose 6-P reductase	Q9FVN7
5205	0.26	.000	TC63232	12438	27094	5.51	5.61	7+4	340	22	3-beta hydroxysteroid dehydrogenase	Q65XW4
5704	0.46	.036	TC51756	35016	76362	6.09	5.59	8+2	80	24	Succinate dehydrogenase	O82663
6416	2.22	.028	TC69306	43514	40639	6.55	5.83	29+7	546	60	Alcohol dehydrogenase 2	Q9FZ01
4313	2.58	.008	TC65374	41001	38628	5.66	5.54	9+1	56	18	Alpha-1 4-glucan-protein synthase	Q9SC19

SSP	P/K	Pval	VvGI5	ThMr	Exp Mr	ThPi	Exp Pi	Pep	Mowse score	% Cov	Annotation	Uniprot
5721	3.21	.006	TC56029	62272	70321	6.09	5.66	14+4	119	30	Pyruvate decarboxylase 1	Q9FVE1
Other proteins												
8114	0.09	.003	TC67872	24602	24225	6.3	6.07	7+6	335	10	20S proteasome alpha subunit F	O82531
214	0.14	.007	TC66224	29540	30609	4.74	4.85	16+5	264	43	14-3-3 protein	Q9LKL0
3601	0.15	.001	TC55206	64597	65725	5.8	5.22	6+3	152	11	Chaperonin-60 beta subunit precursor	P93570
207	0.18	.000	TC52065	24886	32846	4.5	4.75	10+4	268	41	11S globulin-like protein	Q8W1C2
3414	0.31	.013	TC60835	41725	41140	5.31	5.21	8+6	512	16	Actin	Q8H6A3
401	0.35	.013	TC53110[a]	38041	42988	4.62	4.61	11+6	402	25	Ankyrin-repeat protein	Q6TKQ6
3511	0.36	.009	TC53890	46766	44200	5.38	5.38	38+5	258	49	Eukaryotic initiation factor 4A-9	Q40471
3612	0.40	.005	TC55206	60597	64438	5.8	5.73	21+5	137	33	Chaperonin-60 beta subunit precursor	P93570
3009	2.20	.003	TC57670[a]	15352	17695	6.34	5.36	12+5	538	47	Actin-depolymerizing factor 2	Q9FVI1
3308	2.59	.004	TC52033	28429	36906	6.4	5.35	8+1	82	22	Hypothetical protein	Q5AS50
504	3.72	.007	TC57144	42852	40976	4.71	4.68	6+1	103	23	Hypothetical protein (Putative RNA-binding protein)	Q7XXQ8
4504	3.74	.000	TC62003[a]	43130	48804	6.14	5.43	19+5	197	30	Unknown	Q9SUU6
1324	4.74	.024	TC56411	34871	36102	4.89	4.99	18+4	224	39	Ser/Thr protein phosphatase	Q42912
Unidentified proteins												

SSP	P/K	Pval	Exp Mr	Exp Pi	SSP	P/K	Pval	Exp Mr	Exp Pi	SSP	P/K	Pval	Exp Mr	Exp Pi
21	9.65	.033	16187	4.86	2016	3.63	.012	16132	5.15	5418	3.26	.030	39312	5.68
23	0.14	.000	14686	4.76	3108	0.34	.006	26011	5.31	5709	0.38	.040	81132	5.67
24	0.08	.020	14931	4.84	3623	0.43	.042	70437	5.3	5915	5.32	.030	112502	5.69
125	2.84	.036	23615	4.74	4004	0.39	.032	16403	5.49	6004	4.80	.016	16530	5.83
127	10.67	.024	21760	4.64	4201	0.30	.001	27331	5.42	6007	4.85	.031	16569	5.87
131	5.16	042	19973	4.66	5316	3.93	.010	34531	5.62	6008	7.73	.003	16701	5.77
227	7.76	.002	28074	4.65	5317	3.69	.017	34412	5.65	6207	0.25	.015	32782	5.79
1001	0.18	.019	17157	4.91	5318	5.86	.004	34545	5.69	7316	3.66	.027	34091	5.93
1316	4.84	.022	33761	4.89	5412	2.30	.022	40654	5.71	7820	2.57	.011	90326	5.95

[a]Protein spot could be related to other isoforms.

Table 4

Proteins expressed predominantly in seed tissues. SSP, standard spot number; Diff abun, normalized spot volume in the seed and difference in the seed versus pericarp if detected (ratio is indicated in parenthesis) from 12 different plants; VvGI5, match from the translated *Vitis vinifera* gene index Release 5; ThMr, theoretical molecular mass; Exp Mr, experimental molecular mass; ThPi, theoretical isoelectric point (Pi); Exp Pi, experimental isoelectric point (Pi); Pep, number of peptides mass and number of MS/MS ions matching the query; Mowse score; % Cov, percentage of coverage; Annotation, description of protein identity; Uniprot, Uniprot ID of the most closely related Unigene from VvGI5.

SSP	Diff abun	VvGI5	Th Mr	Exp Mr	Th Pi	Exp Pi	Pep	Mowse score	% Cov	Annotation	Uniprot
Globulin TC51863/TC52006 group											
1126	0.10	TC52006	25000	23850	9.99	4.91	6+6	390	16	11S globulin-like protein	Q8W1C2
1128	0.10	TC52006	25000	24797	9.99	4.93	3+3	391	9	11S globulin-like protein	Q8W1C2
1202	0.10	TC52006	25000	27802	9.99	4.73	4+3	279	14	11S globulin-like protein	Q8W1C2
4303	0.10	TC51863	57516	37758	8.37	5.26	6+5	303	42	11S globulin-like protein	Q8W1C2
4504	0.10	TC51863	57516	57885	8.37	5.35	8+2	286	56	11S globulin-like protein	Q8W1C2
7009	0.10	TC51863	57516	18702	8.37	5.82	4+3	201	24	11S globulin-like protein	Q8W1C2
1112	0.11	TC52006	25000	23712	9.99	4.77	6+3	209	10	11S globulin-like protein	Q8W1C2
1118	0.11	TC52006	25000	23804	9.99	4.82	6+4	330	11	11S globulin-like protein	Q8W1C2
3810	0.11	TC52006	25000	111772	9.99	5.16	10+8	772	20	11S globulin-like protein	Q8W1C2
1110	0.11	TC52006	25000	23203	9.99	4.76	5+5	286	14	11S globulin-like protein	Q8W1C2
2401	0.11	TC52006	25000	41967	9.99	4.99	7+5	287	16	11S globulin-like protein	Q8W1C2
1119	0.12	TC52006	25000	23192	9.99	4.82	5+4	363	10	11S globulin-like protein	Q8W1C2
3405	0.12	TC52006	25000	40414	9.99	5.19	6+4	196	13	11S globulin-like protein	Q8W1C2
3811	0.12	TC52006	25000	109517	9.99	5.15	9+7	532	19	11S globulin-like protein	Q8W1C2
1113	0.13	TC52006	25000	24021	9.99	4.77	5+4	403	14	11S globulin-like protein	Q8W1C2
6101	0.13	TC52006	25000	23825	9.99	5.66	5+1	67.1	9	11S globulin-like protein	Q8W1C2
7010	0.13	TC51863	57516	19229	8.37	5.82	5+5	280	24	11S globulin-like protein	Q8W1C2
130	0.15	TC51863	57516	23927	8.37	4.67	5+3	224	10	11S globulin-like protein	Q8W1C2
5002	0.16	TC51863	57516	17865	8.37	5.42	5+5	244	24	11S globulin-like protein	Q8W1C2
3204	0.17 (3.1)	TC51863	57516	30952	8.37	5.29	6+5	489	39	11S globulin-like protein	Q8W1C2
4306	0.17	TC52006	25000	36715	9.99	5.28	7+5	331	16	11S globulin-like protein	Q8W1C2
7007	0.17	TC51863	57516	17515	8.37	5.80	6+6	310	25	11S globulin-like protein	Q8W1C2
7003	0.18	TC51863	57516	18100	8.37	5.80	5+5	233	24	11S globulin-like protein	Q8W1C2

SSP	Diff abun	VvGI5	Th Mr	Exp Mr	Th Pi	Exp Pi	Pep	Mowse score	% Cov	Annotation	Uniprot
136	0.19	TC52006	25000	23079	9.99	4.67	5+4	326	11	11S globulin-like protein	Q8W1C2
3211	0.20	TC51863	57516	30306	8.37	5.21	8+6	456	42	11S globulin-like protein	Q8W1C2
3601	0.20 (9.6)	TC52006	25000	67559	9.99	5.24	11+7	663	21	11S globulin-like protein	Q8W1C2
5004	0.21	TC51863	57516	17524	8.37	5.45	3+3	91.7	16	11S globulin-like protein	Q8W1C2
2607	0.21	TC52006	25000	66685	9.99	5.11	8+5	323	19	11S globulin-like protein	Q8W1C2
2610	0.21	TC52006	25000	70653	9.99	5.08	10+8	683	20	11S globulin-like protein	Q8W1C2
3607	0.22	TC52006	25000	65389	9.99	5.19	6+4	256	13	11S globulin-like protein	Q8W1C2
7008	0.23	TC51863	57516	16276	8.37	5.80	6+6	292	25	11S globulin-like protein	Q8W1C2
7005	0.25	TC51863	57516	16886	8.37	5.80	5+5	219	24	11S globulin-like protein	Q8W1C2
135	0.26	TC52006	25000	23545	9.99	4.67	7+4	319	16	11S globulin-like protein	Q8W1C2
3615	0.26	TC51863	57516	67900	8.37	5.21	8+7	657	42	11S globulin-like protein	Q8W1C2
4205	0.26	TC51863	57516	30014	8.37	5.30	8+7	505	42	11S globulin-like protein	Q8W1C2
3612	0.27	TC52006	25000	69277	9.99	5.12	9+8	679	19	11S globulin-like protein	Q8W1C2
123	0.31	TC51863	57516	25400	8.37	4.67	1+1	77.9	8	11S globulin-like protein	Q8W1C2
2312	0.31 (5.4)	TC51863	57516	31200	8.37	5.20	5+3	143	34	11S globulin-like protein	Q8W1C2
131	0.33	TC52006	25000	24412	9.99	4.67	5+3	302	14	11S globulin-like protein	Q8W1C2
3604	0.33	TC52006	25000	68058	9.99	5.17	8+7	583	19	11S globulin-like protein	Q8W1C2
2301	0.34 (12)	TC51863	57516	31649	8.37	5.09	4+2	108	24	11S globulin-like protein	Q8W1C2
4204	0.62	TC51863	57516	29952	8.37	5.27	8+5	330	42	11S globulin-like protein	Q8W1C2
5202	0.64	TC51863	57516	29326	8.37	5.42	8+6	605	42	11S globulin-like protein	Q8W1C2
1407	0.65	TC52006	25000	39898	9.99	4.89	10+8	774	20	11S globulin-like protein	Q8W1C2
1412	1.45	TC52006	25000	39664	9.99	4.94	6+5	459	13	11S globulin-like protein	Q8W1C2
2309	2.35 (122)	TC52006	25000	37096	9.99	5.22	9+7	709	19	11S globulin-like protein	Q8W1C2
2311	2.57	TC52006	25000	36848	9.99	5.08	9+7	716	19	11S globulin-like protein	Q8W1C2
3316	5.64	TC52006	25000	36947	9.99	5.14	7+5	382	17	11S globulin-like protein	Q8W1C2
Globulin TC51818/TC52065 group											
202	0.10 (2.5)	TC52065	34951	27034	10.26	4.64	7+4	257	30	11S globulin isoform 3	Q8W1C2
1619	0.10 (4.2)	TC52065	34951	66206	10.26	5.07	5+4	303	23	11S globulin isoform 3	Q8W1C2
2210	0.10	TC52065	28618	26633	4.98	5.08	6+5	399	29	11S globulin isoform 3	Q8W1C2
4007	0.10	TC52065	28618	15977	4.98	5.38	4+5	205	17	11S globulin isoform 3	Q8W1C2
2217	0.12	TC51818	40942	30739	5.72	5.10	2+2	184	13	11S globulin-like protein	Q8W1C2

SSP	Diff abun	VvGI5	Th Mr	Exp Mr	Th Pi	Exp Pi	Pep	Mowse score	% Cov	Annotation	Uniprot
5006	0.12	TC52065	34951	18701	10.26	5.43	3+1	72	17	11S globulin isoform 3	Q8W1C2
133	0.13	TC52065	34951	24976	10.26	4.65	8+3	354	21	11S globulin isoform 3	Q8W1C2
134	0.13	TC52065	34951	24446	10.26	4.65	6+4	412	22	11S globulin isoform 3	Q8W1C2
4001	0.13 (7)	TC52065	28618	15399	4.98	5.39	6+5	269	23	11S globulin isoform 3	Q8W1C2
6003	0.13	TC51818	40942	17367	5.72	5.67	6+4	172	11	11S globulin-like protein	Q8W1C2
1116	0.15	TC52065	34951	24938	10.26	4.77	4+4	339	20	11S globulin isoform 3	Q8W1C2
2207	0.15 (5.4)	TC52065	34951	28357	10.26	5.17	6+5	470	25	11S globulin isoform 3	Q8W1C2
6005	0.15	TC51818	40942	16840	5.72	5.67	6+4	324	18	11S globulin-like protein	Q8W1C2
137	0.16	TC52065	34951	22698	10.26	4.67	5+4	499	21	11S globulin isoform 3	Q8W1C2
138	0.16	TC52065	34951	25524	10.26	4.64	2+2	152	8	11S globulin isoform 3	Q8W1C2
1302	0.16	TC52065	28618	36607	4.98	4.73	9+4	336	35	11S globulin isoform 3	Q8W1C2
1221	0.16 (2.2)	TC52065 / TC62049	34951 / 29316	29301	10.26/4.99	4.94	10+5/7+3	511 /256	39 /21	11S globulin isoform 3 / Polyneuridine-aldehyde esterase	Q8W1C2/Q9SE93
5015	0.17 (4.4)	TC51818	40942	16285	5.72	5.67	7+4	309	18	11S globulin-like protein	Q8W1C2
211	0.19	TC52065	34951	26649	10.26	4.69	6+4	325	16	11S globulin isoform 3	Q8W1C2
1306	0.19	TC51818	40942	37198	5.72	4.79	8+6	543	30	11S globulin-like protein	Q8W1C2
3104	0.19	TC52065	34951	26000	10.26	5.16	10+7	515	39	11S globulin isoform 3	Q8W1C2
2604	0.23	TC52065	34951	66091	10.26	5.04	5+4	212	26	11S globulin isoform 3	Q8W1C2
6007	0.25	TC51818	40942	15740	5.72	5.68	8+3	237	21	11S globulin-like protein	Q8W1C2
6009	0.26	TC51818	40942	15204	5.72	5.68	5+4	228	13	11S globulin-like protein	Q8W1C2
2223	0.33 (5)	TC52065	34951	28973	10.26	5.15	5+4	291	15	11S globulin isoform 3	Q8W1C2
1313	0.57	TC52065	34951	36959	10.26	4.82	3+3	137	17	11S globulin isoform 3	Q8W1C2
1315	0.65	TC52065	34951	35753	10.26	4.86	11+7	579	43	11S globulin isoform 3	Q8W1C2
1323	2.37	TC52065	28618	36799	4.98	4.96	11+7	703	48	11S globulin isoform 3	Q8W1C2
1324	5.54	TC52065	28618	36066	4.98	4.91	11+4	489	44	11S globulin isoform 3	Q8W1C2
2314	5.86	TC51818	40942	36651	5.72	5.05	8+6	602	23	11S globulin-like protein	
Other globulins											
1103	0.10	CB34791231578		24720	8.69	4.72	7+5	346	33	11S globulin-like protein	Q8W1C2
1114	0.17	CB34791231578		24330	8.69	4.77	11+5	319	42	11S globulin-like protein	Q8W1C2
2211	0.24	TC58877	43842	27202	5.42	5.10	5+2	96.2	9	11S globulin seed storage protein	Q38712
Other seed storage proteins											
8111	0.12	TC52776	48518	25484	6.74	6.05	10+6	355	18	PreproMP27-MP32	Q39651

SSP	Diff abun	VvGI5	Th Mr	Exp Mr	Th Pi	Exp Pi	Pep	Mowse score	% Cov	Annotation	Uniprot
4003	0.13	TC54826	18424	19150	6.38	5.34	7+5	278	27	Seed maturation protein PM31	Q9XET1
2001	0.20 (5.4)	TC65957	22331	135176	9.03	5.05	1+2	129	17	2S albumin	Q84NG9
2201	0.21	TC52776	48518	26798	6.74	4.97	6+4	139	14	PreproMP27-MP32	Q39651
6103	0.23	TC52776	48518	25173	6.74	5.72	5+3	224	15	PreproMP27-MP32	Q39651
8204	0.38	TC51747	35463	27799	8.74	6.04	28+5	558	31	48-kDa glycoprotein	Q8S4P9
8205	0.52	TC51747	35463	28949	8.74	6.04	15+6	551	15	48-kDa glycoprotein	Q8S4P9
7213	0.53 (4.5)	TC51747	23770	27758	6.53	5.94	17+6	392	21	48-kDa glycoprotein	Q8S4P9
8101	1.02	TC52776	48518	24053	6.74	6.04	11+4	310	22	PreproMP27-MP32	Q39651
Carbohydrate metabolism											
7401	0.12	TC63671	13988	39394	8.85	5.86	3+2	125	20	Steroleosin-B	Q8LKV5
7603	0.12	TC62850	49786	73376	5.54	5.85	11+4	130	17	Glucose-6-phosphate 1-dehydrogenase, cyt	P37830
8415	0.14	TC63091	41054	43306	6.2	6.04	20+7	645	38	Alcohol dehydrogenase 1	Q43690
7416	0.16	TC69306	43715	43030	6.56	5.85	7+4	223	17	Alcohol dehydrogenase 2	Q9FZ01
4624	0.17 (9.7)	TC53291	54243	64648	5.56	5.47	14+7	578	41	Galactokinase	Q9SEE5
5506	0.18 (13)	TC60581	49790	56351	5.8	5.64	24+7	650	48	Enolase 1 (2-phosphoglycerate dehydratase)	Q9LEJ0
7407	0.27	TC52072	42422	42803	6.29	5.92	19+7	553	40	Phosphoglycerate kinase, cytosolic	Q42962
Other metabolism											
5404	0.10	TC61960	39231	42269	5.94	5.56	11+5	340	30	AX110P-like protein	Q9SZ83
4309	0.11	TC51797	33806	36825	5.39	5.32	8+7	360	21	Allergenic isoflavone reductase	Q9FUW6
5513	0.13	TC66898	56548	56616	7.46	5.59	18+7	445	28	Succinate-semialdehyde dehydrogenase	Q2T3E1
9003	0.35	TC59490	11945	12270	8.46	6.23	4+2	137	20	Pru p 1	Q9LED1
Energy											
1209	0.10	TC56895	29382	29127	5.4	4.86	8+7	333	35	Chlorophyll A/B binding protein	Q32291
2609	0.10 (2.6)	TC63054	63793	60032	6.52	5.16	11+4	408	35	ATP synthase beta chain, mitochondrial	P17614
3302	0.17	TC54765	35289	32396	6.08	5.13	11+8	509	35	Oxygen evolving enhancer protein 1	Q9LRC4
Protein fate											
4601	0.12	TC69987	61344	69410	5.85	5.27	18+3	136	51	Chaperonin CPN60-2, mitochondrial	Q05046
4416	0.13 (2.6)	TC56234	41388	40990	5.47	5.54	7+3	224	22	Protein disulfide isomerase	Q6I685
3509	0.14	TC55000	41492	551881	5.1	5.13	10+3	139	23	Mitochondrial processing peptidase alpha subunit	P29677
1321	0.16	TC60801/TC57433	55662/29344	33888	4.99/4.68	4.73	9+5/8+3	291/174	17/22	Aspartic proteinase 3/ 14-3-3	Q9FRW7/P46266
1303	0.29	TC60801	55662	33313	4.99	4.74	8+6	456	16	Aspartic proteinase 3	Q9FRW7

SSP	Diff abun	VvGI5	Th Mr	Exp Mr	Th Pi	Exp Pi	Pep	Mowse score	% Cov	Annotation	Uniprot
Biotic and Abiotic Stress											
6209	0.10	TC52173	56548	27267	7.46	5.60	15+7	348	28	Glutathione-S-transferase	O49235
6210	0.10	TC51718	27557	30390	5.71	5.68	12+2	132	26	Cytosolic ascorbate peroxidase	Q41772
1205	0.11	TC60929	27270	30162	5.38	4.78	3+2	234	8	Class IV chitinase	Q7XAU6
1403	0.11	TC54145	34679	41372	4.66	4.72	14+6	394	37	Salt tolerance protein	Q5PXN9
2713	0.11 (3)	TC70328	71342	77942	5.14	5.12	4+3	172	11	Hsc70 protein,	Q40151
3707	0.11	TC53154	48727	774092	5.02	5.18	12+4	94	14	Heat shock protein 70	Q40693
7106	0.15	TC51764	25284	25328	6.8	5.86	5+3	90.1	12	Superoxide dismutase [Mn], mitochondrial	P11796
3701	0.18	TC53231	71171	75498	5.17	5.14	28+6	633	34	Heat shock cognate protein 70	Q8GSN4
6202	0.24 (3.8)	TC51718	27557	29355	5.71	5.72	3+2	112	11	Cytosolic ascorbate peroxidase	Q41772
7103	0.34	TC51764	28111	25065	6.6	5.89	15+6	420	30	Superoxide dismutase [Mn], mitochondrial	P11796
8103	0.34	TC67773	27081	22470	9.23	6.10	11+3	213	24	P-lip hydroperoxide glutathione peroxidase	O48646
Other proteins											
306	0.11	TC60052	26349	33136	4.77	4.67	12+6	582	52	Late embryogenesis abundant protein D-34	P09444
4507	0.12	TC56794	36730	50787	9.88	5.40	8+3	269	23	Late embryogenesis abundant protein	CAB86908
5509	0.12	TC56794	36730	50215	9.88	5.54	2+1	93	9	Late embryogenesis abundant protein	CAB86908
1309	0.14	TC55192/TC60801	28739/55662	33228	4.79/4.99	4.86	13+6/7+2	244/102	27/16	14-3-3 protein 7/Aspartic proteinase 3	P93212/Q9FRW7
3504	0.29	TC60835	41726	44013	5.31	5.23	19+6	499	27	Actin	Q8H6A3
Unknown proteins											
8112	0.10	CB978962 31781		22379	7.9	6	8+6	362	30	Unknown protein	10178125
4414	0.11	TC54532	40334	43120	5.77	5.33	14+7	399	25	Unknown	CAB02653
7301	0.13	TC57576	21011	31315	5.24	5.84	5+2	60.8	12	Unknown	Q941A4
6206	0.56 (7.6)	TC57394	26532	30143	5.94	5.76	4+1	107	15	Embryo-specific protein	Q9ZNS9
Water-status regulated protein **WW/DS**											
7203	(4.17)	TC58896	26032	28706	6.24	5.88	8+3	123	29	Vacuolar H^+-ATPase, subunit E	Q8SA35
Unidentified proteins											

SSP	Diff abun	Exp Mr	Exp Pi	SSP	Diff abun	Exp Mr	Exp Pi	SSP	Diff abun	Exp Mr	Exp Pi
35	0.10 (9.9)	15007	4.65	132	0.20	24876	4.67	210	0.10	28391	4.69
1115	0.10	25561	4.77	1310	0.14	32449	4.82	2004	0.18	21266	5.11
2015	0.10 (8.7)	14939	5.11	2202	0.15	28412	4.99	2209	0.26 (5.9)	31507	5.16
2215	0.14 (5.9)	30182	5.18	2315	8.11	36997	5	2709	0.15	85731	5.04

SSP	Diff abun	Exp Mr	Exp Pi	SSP	Diff abun	Exp Mr	Exp Pi	SSP	Diff abun	Exp Mr	Exp Pi
3101	0.23 (4.7)	25174	5.26	3613	0.17	67407	5.14	3719	0.38	75761	5.24
4208	0.10	28045	5.35	4402	0.14	42494	5.26	4505	0.15	46339	5.38
5003	0.10	16352	5.44	5101	0.28	24614	5.41	5203	0.10	30143	5.42
5207	0.34	27279	5.56	5304	0.11	33362	5.56	6001	0.20	19465	5.60
6011	0.17	13507	5.74	6108	0.33 (2.4)	24272	5.71	7202	0.49 (3.6)	31176	5.87
7212	0.12 (2.3)	33452	5.93	8001	0.46	17691	5.93	8002	0.23	17713	6.06
8008	0.28	17738	6.18	8302	0.19	37726	6	8416	0.12	43382	6.07

Table 5

Proteins whose abundance was significantly different between well watered and water-deficit in skin. SSP, standard spot number; WW/WD, normalized spot volume in the well-watered skin divided by the normalized spot volume in the water-deficit skin, from 12 different plants; Pval, P value; VvGI5, match from the translated Vitis vinifera gene index Release 5; ThMr, theoretical molecular mass; Exp Mr, experimental molecular mass; ThPi, theoretical isoelectric point (Pi); Exp Pi, experimental isoelectric point (Pi); Pep, number of peptides mass and number of MS/MS ions matching the query; Mowse score; % Cov, percentage of coverage; Annotation, description of protein identity; Uniprot, Uniprot ID of the most closely related Unigene from VvGI5.

SSP	WW/WD	Pval	Vvgi5	Th Mr	Exp Mr	Th Pi	Exp Pi	Pep	Mows score	% cov	Annotation	Uniprot
2318	0.11	.037	TC51818	40942	35857	5.72	5.07	11+5	263	34	11S globulin-like protein	Q8W1C2 .000
822	0.25	.042	TC60724	39345	93831	9.14	4.85	22+4	143	26	Patellin 1	Q2Q0V7
4204	0.29	.040	TC54618	25584	26482	5.51	5.44	14+4	179	34	Proteasome subunit alpha type 2-B	Q8L4A7
5405	0.29	.016	TC42731	15662	43635	5.48	5.63	4+3	66	23	GDP-mannose pyrophosphorylase	Q8W4J5
5215	0.32	.005	TC51718	27557	27714	5.71	5.71	18+6	447	46	Cytosolic ascorbate peroxidase	Q41772
6618	0.34	.018	TC65305	54992	61368	5.80	5.69	18+3	238	45	Neutral leucine aminopeptidase	Q8GZD8
1801	0.42	.003	TC60724	67754	92542	4.72	4.89	14+7	553	18	Patellin 1	Q2Q0V7
7619	0.44	.008	TC54806	58481	59979	6.42	5.89	33+5	372	52	Mitochondrial processing peptidase beta sb	Q9AXQ2
5109	0.45	.032	TC68818	29626	25805	6.71	5.62	7+6	322	21	20S proteasome beta subunit PBB2	O81152
7313	2.07	.024	TC57431	35488	37683	6.18	6.03	22+3	182	53	Cytosolic malate dehydrogenase	Q9FT00
3220	2.36	.049	TC55034	25124	28931	5.26	5.31	11+7	561	36	Chalcone isomerase	P51117
5102	2.57	.041	TC51878	27794	23592	8.33	5.56	13+6	386	36	Oxygen-evolving enhancer 2 chloroplast	Q9SLQ8
5501	3.10	.033	TC69652	40193	44173	5.63	5.55	20+1	62	57	Leucoanthocyanidindioxgenase	P51093
3313	7.36	.008	TC45122	29869	33325	5.15	5.23	4+3	130	13	Cyclase	Q2I313
Unidentified proteins												

SSP	WW/DS	Pval	Exp Mr	Exp Pi	SSP	WW/DS	Pval	Exp Mr	Exp Pi	SSP	WW/DS	Pval	Exp Mr	Exp Pi
3118	4.990	.024	22455	5.32	6422	2.392	.041	39246	5.88	7103	3.246	.020	22627	5.90
7911	3.996	.003	111063	5.99										

Table 6

Proteins whose abundance was significantly different between well watered and water-deficit in pulp. SSP, standard spot number; WW/WD, normalized spot volume in the well-watered pulp divided by the normalized spot volume in the water-deficit pulp, from 12 different plants; Pval, P value; VvGI5, match from the translated *Vitis vinifera* gene index Release 5; ThMr, theoretical molecular mass; Exp Mr, experimental molecular mass; ThPi, theoretical isoelectric point (Pi); Exp Pi, experimental isoelectric point (Pi); Pep, number of peptides mass and number of MS/MS ions matching the query; Mowse score; % Cov, percentage of coverage; Annotation, description of protein identity; Uniprot, Uniprot ID of the most closely related Unigene from VvGI5.

SSP	WW/WD	Pval	VVGI5C	ThMr	Exp Mr	ThPi	Exp Pi	Pep	Mowse score	% cov	Annotation	Uniprot
4303	0.26	.017	TC55139/TC51797	33809	35211	5.39	5.43	9+3 / 7+3	139 /131	22 /20	Glyoxalase I, partial (92%) / Allergenic isoflavone reductase Bet v6.0102	Q9ZWJ2/Q9FUW6
5619	0.29	.038	TC54345	57126	64508	5.51	5.72	22+5	168	32	Glutamate decarboxylase	P54767
220	0.42	.027	TC57433	29344	29904	4.68	4.77	15+4	331	39	14-3-3 protein	P46266
3113	0.43	.048	TC68794	27224	24074	5.38	5.37	2+2	244	11	Class IV endochitinase	Q7XAU6
8602	2.26	.004	TC57645	54492	60444	7.04	6.05	36+7	549	59	UDP-glucose pyrophosphorylase	Q8W557
6119	2.27	.025	TC63472	18147	18729	6.17	5.81	10+4	146	20	18.6 kDa heat-shock protein	Q39929
504	2.89	.016	TC57144	42853	40976	4.71	4.68	6+1	103	23	Latex abundant protein	Q6XNP6
3613	2.93	.023	TC56912	30947	65458	5.92	5.35	17+3 / 16+3	174	42 / 66	Vacuolar H+-ATPase A / UDP-glucose pyrophosphorylase	Q9MB47/17026394
6715	4.51	.016	TC52137	84537	85179	6.09	5.86	7+3	144	15	Methionine synthase	Q42662

Unidentified proteins

SSP	WW/WD		Exp Mr	Exp Pi	SSP	WW/DS		Exp Mr	Exp Pi	SSP	WW/DS		Exp Mr	Exp Pi
4117	3.37	.023	21273	5.46	4805	0.30	.046	88278	5.46	5113	2.9	.035	22663	5.65